Chem Soc Rev

Molecular artificial photosynthesis

Q1 Q2

Serena Berardi,[a] Samuel Drouet,[a] Laia Francàs,[a] Carolina Gimbert-Suriñach,[a] Miguel Guttentag,[a] Craig Richmond,[a] Thibaut Stoll[a] and Antoni Llobet*[ab]

The replacement of fossil fuels by a clean and renewable energy source is one of the most urgent and challenging issues our society is facing today, which is why intense research has been devoted to this topic recently. Nature has been using sunlight as the primary energy input to oxidize water and generate carbohydrates (a solar fuel) for over a billion years. Inspired, but not constrained, by nature, artificial systems can be designed to capture light and oxidize water and reduce protons or other organic compounds to generate useful chemical fuels. This tutorial review covers the primary topics that need to be understood and mastered in order to come up with practical solutions for the generation of solar fuels. These topics are: the fundamentals of light capturing and conversion, water oxidation catalysis, proton and CO_2 reduction catalysis and the combination of all them for the construction of complete cells for the generation of solar fuels.

Key learning points
(1) Photosynthesis and artificial photosynthesis.
(2) Light harvesting molecules and materials.
(3) Water oxidation catalysis.
(4) Proton reduction catalysis.
(5) CO_2 reduction catalysis.
(6) Photoelectrochemical cells for the production of solar fuels.

1. General introduction

In view of depleting fossil fuels and the concomitant drastic pollution of the environment, considerable attention is directed towards finding alternative, more sustainable and recyclable ways to store and distribute energy.[1] Existing alternatives such as solar panels, wind-, tidal- or hydroelectric-power plants are widely used but have the disadvantage of providing the converted energy in the form of electricity, which is difficult to store and transport. Therefore, an alternative chemical form of energy carriers, similar to fossil fuels, is highly desirable.

The only real and inexhaustible energy source available on our planet is from the sun. Fossil resources are in fact stored sunlight, which was emitted by our sun millions of years ago and converted by plants into high energy chemicals. Upon anaerobic fermentation, these substances were

converted into the fossil energy resources used today. Unfortunately, since the process of plants storing sunlight in chemicals and the subsequent fermentation take several millions of years, it can neither be considered recyclable, nor can it meet the rate of energy consumption of our society. However, the principle idea of storing sunlight in chemical bonds can serve as a great inspiration in the search for alternative energy carriers.

In nature plants convert sunlight into chemically accessible energy by absorbing photons with photosystem II (PSII) in chloroplasts, which results in a charge separation (or electron–hole pairs) and gives the system the necessary power to perform redox-reactions (Scheme 1). The oxidative holes are used to activate the oxygen evolving centre (OEC) which in turn oxidises water to molecular oxygen. The electrons pass through a second photosystem (PSI) and finally serve to produce energetically enriched bio-reducing agents such as NADPH or ATP. These are further used in the Calvin cycle to ultimately reduce atmospheric carbon dioxide to a variety of carbohydrates, nature's carbon based fuel. Upon metabolization of these natural energy carriers their energy content is released and

Q4 [a] Institute of Chemical Research of Catalonia (ICIQ), Avinguda Països Catalans, 16, 43007 Tarragona, Spain
[b] Departament de Química, Universitat Autònoma de Barcelona, Cerdanyola del Vallès, 08193 Barcelona, Spain

This journal is © The Royal Society of Chemistry 2014

Chem. Soc. Rev., 2014, 00, 1–19 | 1

CO₂ is regenerated. This system is therefore perfectly cycled and accordingly sustainable.

The concept of storing the sun's energy in chemical bonds can be used to construct an artificial photosynthetic system: water is oxidised to oxygen and the electrons are either used to reduce CO_2 to methane, methanol, formaldehyde, formate, carbon monoxide or oxalate, or they are used to reduce protons to hydrogen (Table 1). In each of these cases the resulting chemicals have a higher energetic content and have all the properties of a fuel, *e.g.* they can be stored, transported and burned to release their energy content.

To be able to perform artificial photosynthesis and make the process kinetically viable, different components are needed to perform each of the steps of the reaction, *e.g.* the absorption of light, the oxidation of water and the reduction of either CO₂ or protons (Scheme 2). Since the entire reaction is very complicated and only a handful of artificial systems are known to produce O_2 and H_2 simultaneously, a useful strategy is to divide the overall process into its two half reactions, the oxidative O₂ evolving reaction and the reductive H_2 evolving (or CO₂ reducing) reaction. In both half reactions the corresponding half reaction is mimicked by a sacrificial redox agent (sacrificial electron donor, SED or sacrificial electron acceptor, SEA) in order to provide the required electrons or oxidative equivalents. This separation facilitates greatly the study and optimization of the catalysts and enables detailed investigations, avoiding undesired back- and side-reactions. Once each side is optimised under homogeneous conditions, the half reactions are in
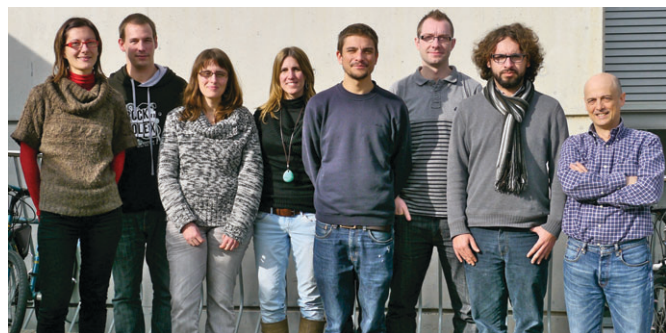
Serena Berardi

Serena Berardi graduated in Chemistry in 2006 at the University of Rome "Tor Vergata". She earned her PhD from the University of Padova in 2010 under the supervision of Prof. Scorrano and Dr Bonchio. After two years of post-doctoral research in the same group, she moved to Ferrara, to work in the team of Prof. Bignozzi and Dr Argazzi. In June 2013 she joined the group of Prof. Llobet at the ICIQ as a post-doctoral researcher. She is currently involved in the investigation of new catalytic systems for photo-induced water oxidation, as well as in the development of photoanodes.

Samuel Drouet received his PhD in Molecular Chemistry from the University of Rennes in 2010 under the supervision of Dr Christine Paul-Roth. He then joined the Laboratory of Molecular Electrochemistry at the Université Paris Diderot as a Postdoctoral Research Associate for two years, under the guidance of Profs. Cyrille Costentin, Marc Robert and Jean-Michel Savéant. Samuel is currently working on his second postdoctoral fellowship at ICIQ in the group of Prof. Antoni Llobet. His research interests are centered on the synthesis and the studies of organometallic complexes for the activation of small molecules toward the production of sustainable fuels.

Laia Francàs Forcada graduated in Chemistry at Autonomous University of Barcelona (UAB) in 2006. She earned her PhD from the same university in 2011, under the direction of Dr Lluís Escriche, Dr Xavier Sala and Prof. Antoni Llobet investigating molecular catalysts for water oxidation. Then she moved to Institute of Chemical Research of Catalonia (ICIQ) as a project researcher in the group of Prof. Antoni Llobet. She is currently involved in the development of water splitting systems, focusing on the photoanodes.

Carolina Gimbert Suriñach obtained her PhD from the Autonomous University of Barcelona (UAB) in 2008, under the supervision of A. Vallribera. After one year as an assistant professor in the same university, she moved to the University of New South Wales (UNSW) to undertake post-doctoral research with S. B. Colbran. In 2012 she joined A. Llobet's team at the Institute of Chemical Research of Catalonia (ICIQ) to work on hydrogen evolving photocatalysis for water splitting.

Miguel Guttentag received his bachelor's and master's degrees from the University of Zurich, obtaining the Alfred Werner award in 2005, 2007 and 2008. He obtained his PhD at the same university under the supervision of Prof. Roger Alberto in 2013 investigating molecular catalysts for hydrogen evolution. In May 2013 he joined the group of Prof. Antoni Llobet at the ICIQ as a Postdoctoral Researcher where he tries to combine hydrogen and oxygen evolving reactions into one photocatalytic water splitting system.

Craig Richmond obtained his MSci degree in Chemistry with Medicinal Chemistry with Work Placement from the University of Glasgow in 2006, after which he was awarded the John L. T. Waugh Prize for Chemistry and a University of Glasgow Scholarship to continue his predoctoral studies under the supervision of Prof. Lee Cronin. After a short postdoctoral stay in the same lab he then moved to the group of Prof. Antoni Llobet at ICIQ in 2011 with a Marie Curie Intra-European Fellowship. Here his current interests are focused on the design and evaluation of novel ruthenium based catalysts for water oxidation.

Thibaut Stoll completed his master's degree in nanochemistry and nano-objects from the Joseph Fourrier University in Grenoble, France, in 2009. He obtained his PhD in 2012 from the Grenoble University under the direction of Dr Marie-Noëlle Collomb in the field of electro and photocatalytical hydrogen production from water using coordination complexes. Thibaut joined the group of Prof. Antoni Llobet, at the ICIQ, in February 2013 as a project researcher and currently investigates the interactions and synergies of coordination complexes and semi-conductors for water splitting applications.

Antoni Llobet received a PhD from UAB. Then he was a Postdoctoral Fellow at the University of North Carolina with T. J. Meyer and at Texas A&M University with D. T. Sawyer and A. E. Martell. He is currently a Professor of Chemistry at UAB and a Group Leader at ICIQ.

2 | *Chem. Soc. Rev.,* 2014, **00**, 1–19

This journal is © The Royal Society of Chemistry 2014
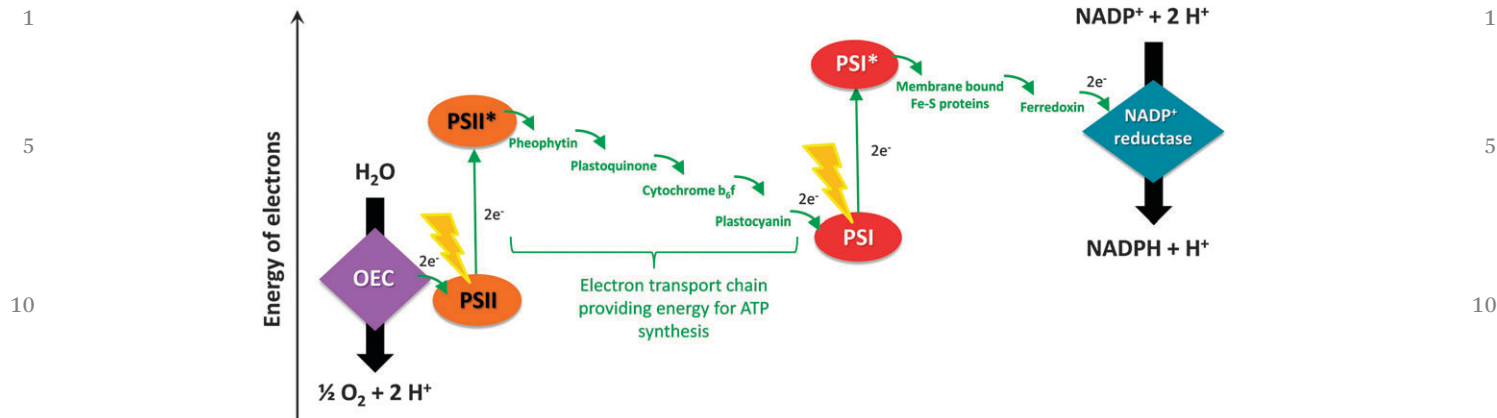
Scheme 1 Schematic representation of photosynthesis with light absorber units PSI and PSII, electron transport chain, oxygen evolving centre (OEC) and NADP$^+$ reductase.

Table 1 Electrochemical reaction equations (all potentials *vs.* NHE at pH 7)

H$_2$O oxidation/H$^+$ reduction		CO$_2$ reduction	
Reaction	$E^{0'}$	Reaction	$E^{0'}$
$H_2O \rightarrow HO^\bullet + 1H^+ + 1e^-$ (1)	2.39	$CO_2 + 1e^- \rightarrow CO_2^{\bullet-}$ (6)	-1.9
$2H_2O \rightarrow HOOH + 2H^+ + 2e^-$ (2)	1.37	$CO_2 + 2H^+ + 2e^- \rightarrow HCO_2H$ (7)	-0.61
$2H_2O \rightarrow HOO^\bullet + 3H^+ + 3e^-$ (3)	1.26	$CO_2 + 2H^+ + 2e^- \rightarrow CO + H_2O$ (8)	-0.53
$2H_2O \rightarrow O_2 + 4H^+ + 4e^-$ (4)	0.81	$2CO_2 + 2H^+ + 2e^- \rightarrow H_2C_2O_4$ (9)	-0.49
		$CO_2 + 4H^+ + 4e^- \rightarrow HCHO + H_2O$ (10)	-0.48
$2H^+ + 2e^- \rightarrow H_2$ (5)	-0.41	$CO_2 + 6H^+ + 6e^- \rightarrow CH_3OH + H_2O$ (11)	-0.38
		$CO_2 + 8H^+ + 8e^- \rightarrow CH_4 + 2H_2O$ (12)	-0.24
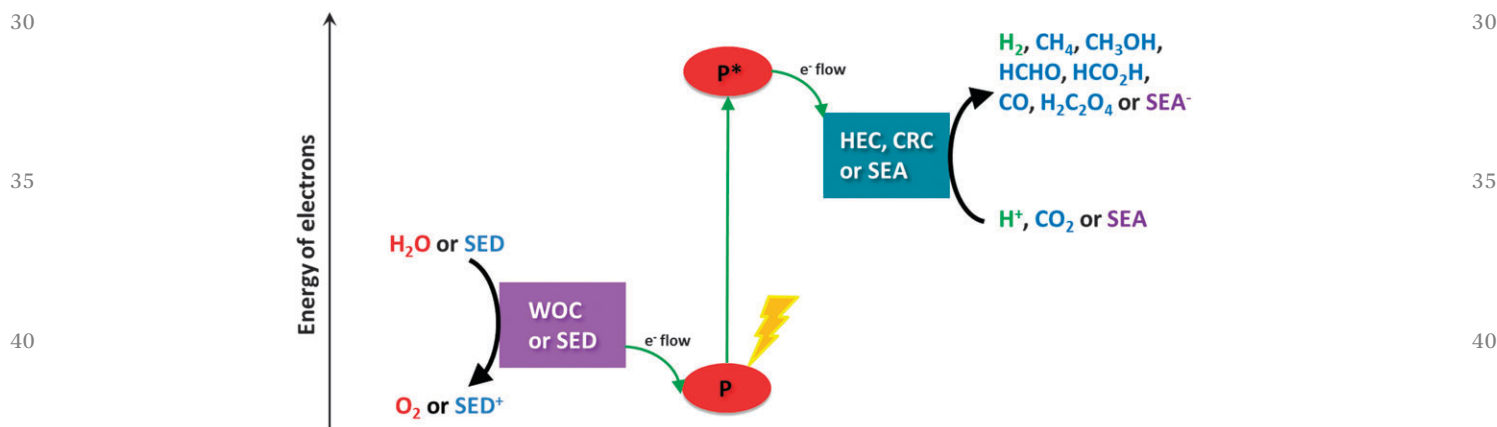
Scheme 2 Generalised schematic representation of artificial photosynthesis with light absorbing unit (P), water oxidation catalyst (WOC) or sacrificial electron donor (SED), hydrogen evolving catalyst (HEC), CO$_2$ reducing catalyst (CRC) or sacrificial electron acceptor (SEA).

principle ready to be heterogenised (*e.g.* onto electrodes) and combined in a full catalytic system as a photoelectrochemical cell (PEC). There are however major challenges to overcome when connecting the half reactions, apart from stability and durability issues, chemical and kinetic conditions for the two reactions need to be matched. The large excess of sacrificial redox agents in the half reactions and their typically irreversible nature provide a driving force for the forward electron transfer. In full systems however, this driving force is missing and back electron transfers (shortcuts) as well as mismatching kinetics

and undesired side products often hinder a productive forward electron flow (for further details see Section 6.5).

In this tutorial review we will present an overview of the most important and most recent advances in each of the half reactions. The review will focus *on molecular systems or immobilised molecular systems* (heterogeneous systems will not be discussed in detail) and is divided accordingly into light absorbing molecules (P), water oxidation catalysts (WOCs),[2] hydrogen evolving catalysts (HECs)[3,4] and CO$_2$ reduction catalysts (CRCs).[5] In the last chapter an overview will be given for

This journal is © The Royal Society of Chemistry 2014

Chem. Soc. Rev., 2014, **00**, 1–19 | **3**

the few systems where the two half reactions have been combined to form a full water splitting system.[2,6,7]

2. Light harvesting systems

2.1. Introduction

Materials and molecules interact with light by three main physical processes, reflection, refraction and absorption. Materials that absorb light do so because the wavelength of light being absorbed is of sufficient energy to promote an electron from a low energy molecular orbital (ground state) to a higher energy orbital (excited state). The wavelength at which a material absorbs will be dependent upon the energy gap between the ground state and the excited state, which is what gives different materials their distinctive colours: Materials that absorb light in the visible region of the electromagnetic spectrum (*ca.* 400–700 nm) will appear coloured whilst those that absorb in the ultraviolet or infrared regions appear colourless. In the majority of cases the energy absorbed is eventually expelled as heat (non-radiative decay) or light (radiative decay) as the excited electron relaxes back to its original state, however some materials, such as semiconductors, can use the potential energy of the excited electron to do work in the form of electrical current or electrochemical transformations. The conversion of solar energy directly to electrical energy is termed photovoltaics whilst the conversion of solar energy to chemical energy is called photosynthesis; both research fields are vital in the search for solar based energy production.

2.2. Photovoltaics

2.2.1. Solar cells. Solar cells, or photovoltaic cells, are devices that generate an electric output under light irradiation. A semiconductor, typically crystalline silicon, absorbs visible light to promote an electron from the low energy valence band (VB) to the higher energy conduction band (CB), creating an electron–hole pair. This electron–hole pair is then transported through an electrical circuit where it can be used to power an electronic device, similar to a battery. The efficiency of a photovoltaic device is highly dependent upon the semiconductor material(s) from which it is made, as well as the physical device morphology and manufacturing techniques. Since the first crystalline silicon solar cells were introduced to the market over 40 years ago, advances have been steady and improvements in solar to electric efficiency have increased from <1% to >40% for today's state-of-the-art multi-junction GaInP/GaInAs/Ge cells.[8] The benefits of sourcing electricity from photovoltaic cells include large device lifespans (>20 years for most commercial solar panels) and relatively low pollution and operating costs; however these are offset against the high material and processing costs during manufacturing and the reliance on solar flux *i.e.* electricity is only produced during the day. Although the problem of inconsistent solar flux cannot be easily overcome, manufacturing costs are constantly falling as demand increases and new technologies are developed, with claims that the price of solar power has already reached parity
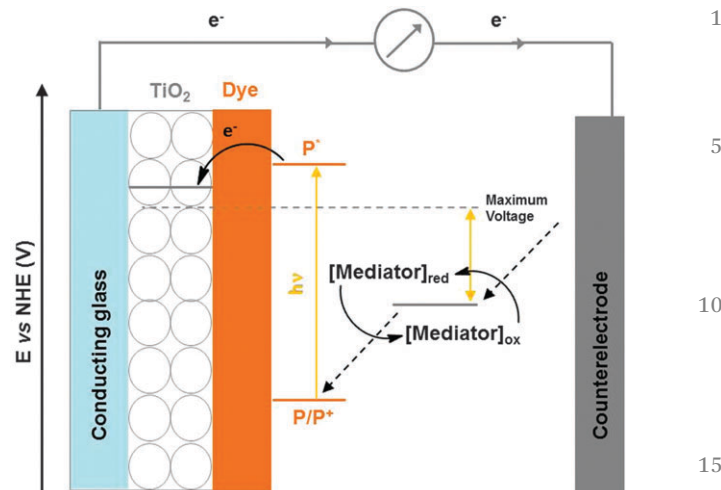
Fig. 1 Structure and operating principle of a typical DSSC.

with grid power in some countries.[9] Thin film solar cells, multiple junction solar cells, organic/polymer solar cells, Quantum Dot Solar Cells (QDSCs), and Dye Sensitised Solar Cells (DSSCs)[10,11] are the main device designs under investigation that are beginning to compete with traditional semiconductor solar cells and ultimately lowering the cost of solar energy.

2.2.2. Dye sensitized solar cells. O'Regan and Grätzel first demonstrated the concept of low cost, high efficiency solar cells in 1991 using a charge-transfer ruthenium dye adsorbed on a film of nanostructured titanium dioxide (TiO_2) semiconductor and an iodide/triiodide redox mediator.[12] A schematic of the generic design of a DSSC can be seen in Fig. 1. The key principles of the cell are light absorption and initial charge separation by the dye molecule (eqn (13)), followed by charge stabilisation through rapid electron injection into the TiO_2 conduction band (eqn (14)) and dye regeneration by the iodide (eqn (15)), and finally reduction of triiodide at the counter electrode completes the cycle (eqn (16)).

$$TiO_2-P + h\nu \rightarrow TiO_2-P^\star \qquad (13)$$

$$TiO_2-P^\star \rightarrow TiO_2(e^-)-P^+ \qquad (14)$$

$$2TiO_2(e^-)-P^+ + 3I^- \rightarrow 2TiO_2(e^-)-P + I_3^- \qquad (15)$$

$$I_3^- + 2e^- \rightarrow 3I^- \qquad (16)$$
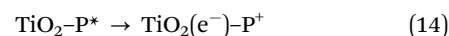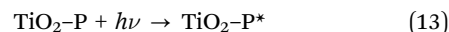
The initial design of DSSCs has changed very little with time however advances with respect to semiconductor morphology, dye structure, redox mediator and electrolyte composition have led to increases in power conversion efficiency from 7.1% to the current value of 15%. This new record breaking device is a solid state DSSC and utilises a $CH_3NH_3PbI_3$ perovskite dye to sensitize the TiO_2 semiconductor and a complex blend of organic and inorganic molecules as the hole-transporting material (HTM) that connects the photoanode to the cathode.[13]

4 | *Chem. Soc. Rev.,* 2014, **00**, 1–19

This journal is © The Royal Society of Chemistry 2014

2.3. Photoelectrodes for water splitting

2.3.1. Semiconductor electrodes. As mentioned previously, photovoltaic devices alone cannot provide the solution to the impending energy crisis due to the current lack of viable methods for transportation and storage. Using solar energy to release hydrogen and oxygen from water would provide a fuel based energy vector that is clean and renewable and is also easily integrated with current transport infrastructure. The photolysis of water with TiO_2 was first demonstrated by Honda and Fujishima in 1972, where with a small electrical bias and irradiation with UV light they succeeded in liberating hydrogen gas and oxygen gas from water.[14] The reason for using high energy UV light in this system was because the energy band gap for TiO_2 is 3.0–3.2 eV, which corresponds to absorbance only in the UV region of <400 nm. Despite this drawback TiO_2 is still by far the most studied semiconductor in artificial photosynthesis: lower energy band gap semiconductors such as Haematite (α-Fe_2O_3) and Cadmium Selenide (CdSe) exist however they either lack the photostability of TiO_2 and/or have band edges that are not appropriate for water splitting.[10,15] See Fig. 2 for a selection of common semiconductors and their relative band positions.

An ideal semiconductor is therefore cheap to manufacture and easily sourced, has a high photochemical stability and a band gap of 1.6–2.4 eV. Until now no such material has been discovered but some ingenious systems have been developed which are able to work around some of these problems.

2.3.2. Anchored dyes and dyads. In a similar fashion to the dye sensitisation of semiconductors for use in photovoltaic cells, dye molecules can be used in conjunction with molecular catalysts for photocatalytic water splitting. A host of molecular catalysts exist for both water oxidation and proton reduction and will be discussed later in Sections 3 and 4, respectively. These catalysts can be adsorbed onto a semiconductor surface in addition to a photosensitiser dye. When the latter is covalently linked to the catalyst, the resulting complex is known as a dyad (D), which can be similarly adsorbed on the semiconductor surface. The photoelectrodes created work in a similar fashion to DSSCs except that in place of mediation by iodide/triiodide the dye regeneration step is carried out by the catalyst and the catalyst is subsequently regenerated by the relative catalytic cycle. Fig. 3 shows some example structures of photosensitiser dyes (P) and dyads (D) that have been used in the development of molecular based photoelectrodes. The overall concept forms a Photoelectrochemical Cell (PEC), the working of which will be discussed in Section 6.

2.4. Homogeneous photoelectrocatalytic systems

Sometimes when studying the interactions of catalyst–photosensitiser systems, more information can be gained from complementary homogeneous studies in addition to studying the heterogeneous electrode setup. In such cases the water splitting reaction is simplified into its half reactions, focussing solely on the relevant half reaction, the other half reaction is replaced by an easier and faster redox reaction by employing a SEA or SED. A suitable photosensitiser for water oxidation must have strong absorbance in the visible spectrum, long excited-state lifetimes at room temperature and a high oxidation potential (high enough to oxidise the WOC). The $[Ru(bpy)_3]^{2+}$
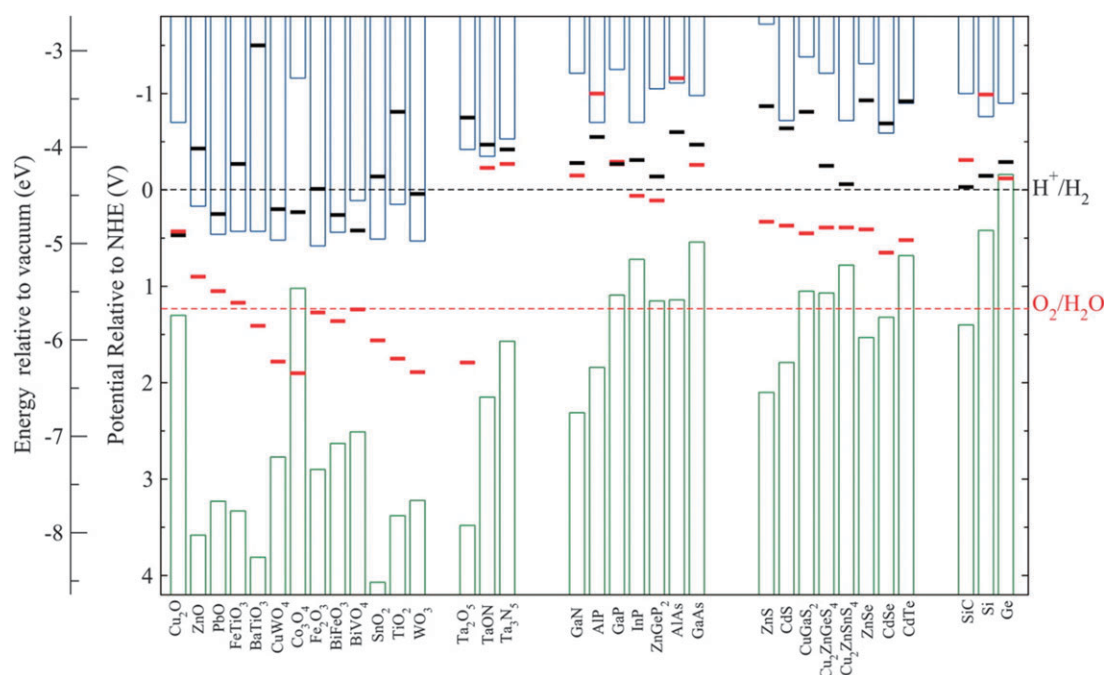
Fig. 2 Calculated oxidation potential E_{ox} (red bars) and reduction potential E_{red} (black bars) relative to the NHE and vacuum level for a series of semiconductors in solution at pH 0, the ambient temperature 298.15 K, and pressure 1 bar. The water redox potentials $E(O_2/H_2O)$ and $E(H^+/H_2)$ (dashed lines) and the valence (green columns) and conduction (blue columns) band edge positions at pH 0 are also plotted. Reprinted with permission from ref. 16. Copyright 2012 American Chemical Society.[16]

This journal is © The Royal Society of Chemistry 2014

Chem. Soc. Rev., 2014, 00, 1–19 | 5
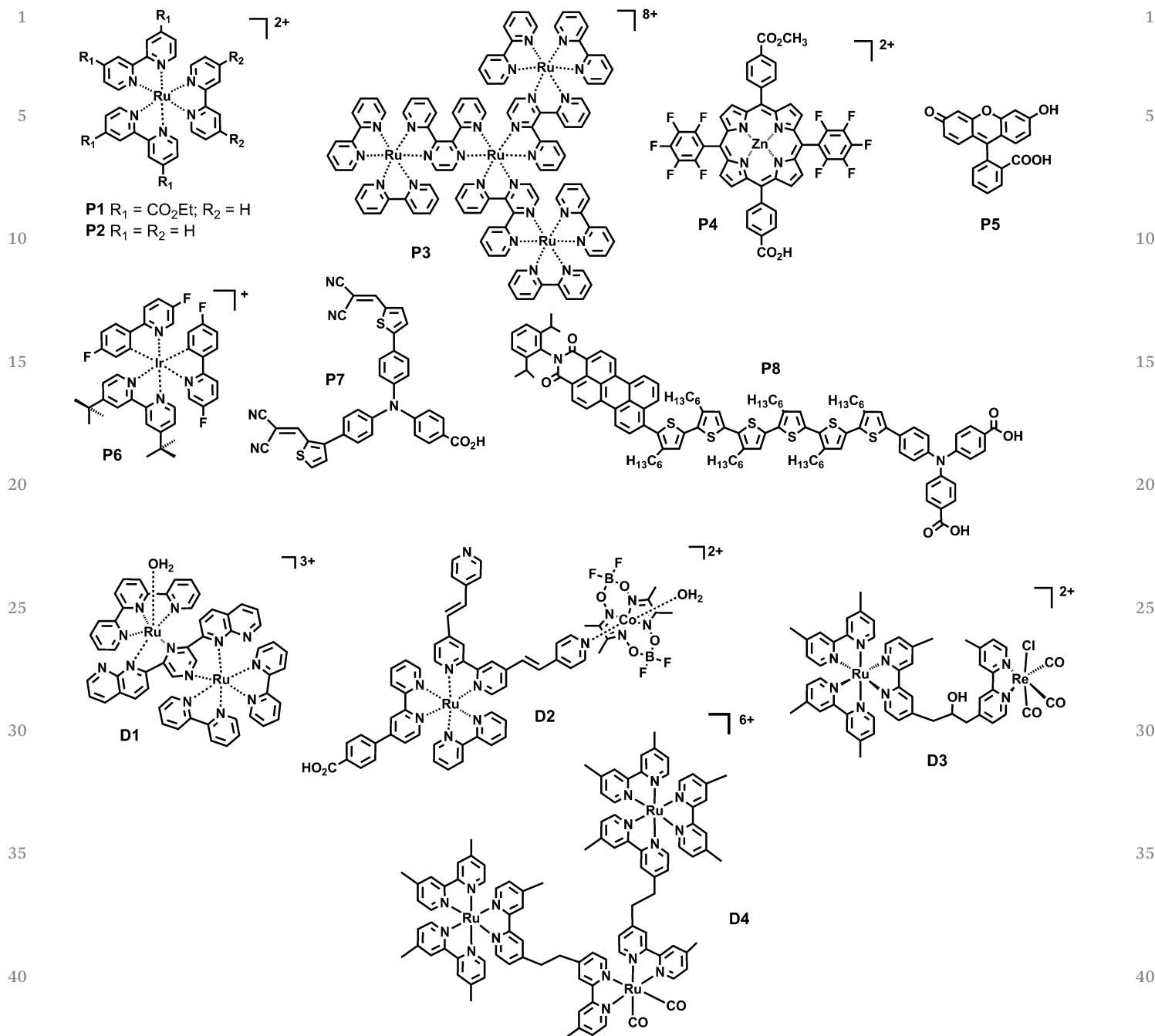
Fig. 3 A selection of photosensitiser dyes (P) and dyad molecules (D).

family (**P1** and **P2** in Fig. 3, bpy = 2,2′-bipyridyl) members are used almost exclusively in this application because they have all of the above-mentioned characteristics: when light is shined on $[Ru(bpy)_3]^{2+}$, the excited state generated, $[Ru(bpy)_3]^{2+*}$, is capable of transferring an electron to a SEA such as $[Co(NH_3)_5Cl]^{2+}$ or $Na_2S_2O_8$ and subsequently forming the strong oxidant, $[Ru(bpy)_3]^{3+}$ *in situ*. The $[Ru(bpy)_3]^{3+}$ should then be capable of oxidising the WOC from its low oxidation state to its active higher oxidation state, which in turn oxidises water to dioxygen.[2,17,18] $[Ru(bpy)_3]^{2+}$ and its analogues are somewhat unique in that they can be used as photosensitisers for both water oxidation and water reduction. When $[Ru(bpy)_3]^{2+}$ is

employed in a homogeneous water reduction system, the photo-generated $[Ru(bpy)_3]^{2+*}$ can receive an electron from a SED such as triethanolamine and form the strong reductant $[Ru(bpy)_3]^{+}$. The HEC is then subsequently reduced to its active oxidation state which in turn begins the catalytic reduction of protons.[3]

3. Water oxidation

3.1. Introduction

Water oxidation is one of the bottlenecks for the successful development of an overall water splitting cell with sunlight.
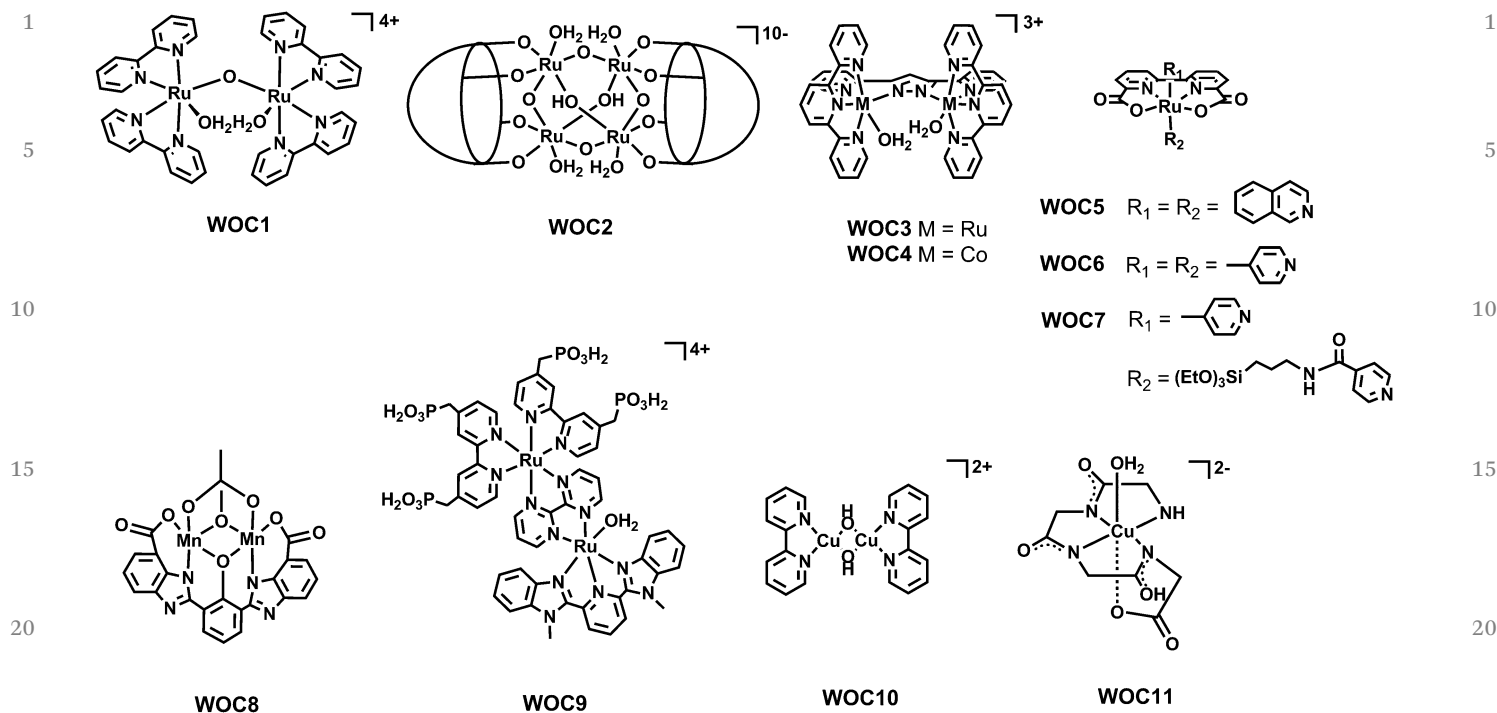
Fig. 4 A selection of water oxidation catalysts. For **WOC2**, the schematically represented ligands are the polyoxometalate $[\gamma\text{-SiW}_{10}\text{O}_{36}]^{8-}$.

Water oxidation is a thermodynamically demanding reaction as can be seen in eqn (1)–(4) of Table 1. The lowest energy path, eqn (4), involves the removal of $4H^+$ and $4e^-$ together with the generation of an O–O bond, reflecting its mechanistic complexity. Currently, there are a number of oxides capable of catalysing the water oxidation reaction, although in general they are orders of magnitude slower than their molecular counterparts.

The field of molecular WOCs benefits from the capacity of the molecular tool to: (i) rationally design WOCs performance based on ligand modifications, choice of transition metal, oxidation state and geometry, through space interactions, electronic coupling, and active site hindering; (ii) increase the solubility by adding additional functionalities; and (iii) enable the anchoring of the catalyst onto electrodes.

Since 1982, when the first well characterised molecular WOC (the so-called "blue dimer", **WOC1** in Fig. 4) was reported, a significant number of WOCs have been synthesised, including mononuclear and polynuclear transition metal complexes.[2] From this existing body of WOCs, a few common features have emerged that allow designing fast and efficient WOCs with long-term stability: first of all, the metal centre(s) must have easy access to high oxidation states that should be stabilised by the ligand framework. The stabilisation of these high oxidation states is generally achieved by Proton Coupled Electron Transfer (PCET), thus avoiding highly charged intermediates. For this purpose, an aquo ligand or an available coordination site to bind a water molecule is essential. This requirement is also crucial in order to generate the M–O group, responsible for the critical O–O bond formation step. Secondly, given the high thermodynamic energy associated with the water oxidation process (0.81 V vs. NHE, Table 1), it is imperative that the ligands

used are oxidatively robust. In addition, the ligands should not suffer easy ligand substitution by solvent water molecules under the working conditions. If either of these two processes occur, the nature of the actual catalyst will be unknown, since the initial molecular catalyst could be transformed to another species or even all the way to the corresponding metal oxide.[19]

3.2. Water oxidation mechanisms

There are two different mechanisms that can operate in the oxygen–oxygen bond formation step:

(i) WNA: Water nucleophilic attack, where a water molecule from the solvent attacks the oxo group from the M–O moiety (Scheme 3). This mechanism can take place when the M–O fragment is electrophilic enough to be attacked by a nucleophilic water solvent molecule. The O–O bond is the result of the interaction between the HOMO of the water molecule and the LUMO of the metal–oxo (M–O) complex. The subsequent cleavage of the M–O bond forms O_2 and the reduced metal centre.[2,20] Most mononuclear WOCs and some polynuclear WOCs, such as **WOC1** and the tetranuclear polyoxometalate **WOC2** are reported to oxidise water through this mechanism.[2]

(ii) I2M: Interaction between two M–O entities, which can be a radical coupling or a reductive elimination. The latter depends on the oxidation state of the metal centre and on the number of oxygens (Scheme 3). As the name indicates, this pathway consists of the interaction of two metal–oxo moieties and, as in the previous case and it can take place both in an *intra*- and in an *inter*-molecular manner. The dinuclear complex **WOC3** undergoes water oxidation through this mechanism by the *intra*-molecular interaction of the two Ru=O moieties, which are perfectly oriented for this interaction. On the other

This journal is © The Royal Society of Chemistry 2014

Chem. Soc. Rev., 2014, **00**, 1–19 | 7
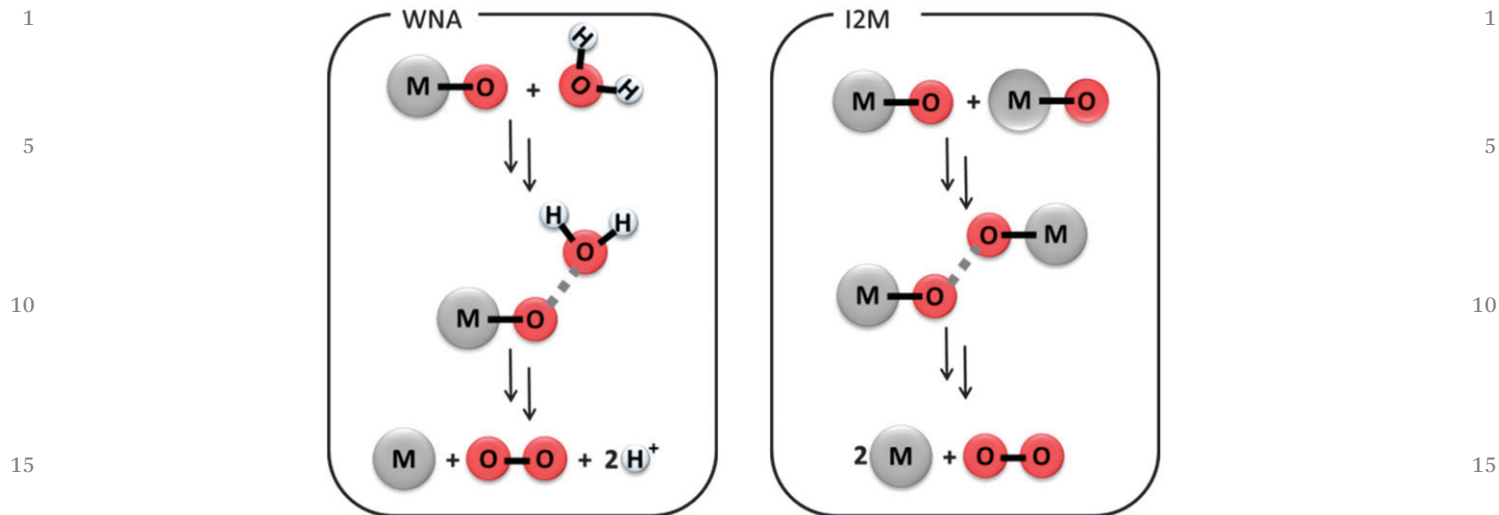
Scheme 3 Potential pathways to form an O–O bond promoted by transition metal complexes. Left, water nucleophilic attack (WNA). Right, interaction between two M–O entities (I2M).

hand, the highly active mononuclear ruthenium complex **WOC6** promotes the oxygen–oxygen bond formation by an *inter*molecular interaction between two complexes (see Section 3.3.1).

These two mechanisms have also been proposed to occur in the oxygen evolving centre of photosystem II (OEC-PSII) in the green plants and algae.[2] The participation of redox active ligands, such as semi-quinones, in the overall water oxidation reaction, has also been proposed by Fujita, Muckerman and coworkers.[21]

3.3. Benchmarks

Before the O–O bond forming step, the WOC must be activated. This activation involves a combination of electron(s) and proton(s) removal (PCET) from the initial M–OH$_2$ active group in order to reach a sufficiently reactive species. The latter can be generated either using a chemical oxidant, by applying an external potential, or using sunlight energy.

3.3.1. Chemically induced WO. The best catalyst described until now is a mononuclear ruthenium catalyst **WOC5** capable of achieving a turnover number of 50.000 (TON), with a turnover frequency (TOF) of 300 s^{-1} using Ce(IV) ((NH$_4$)$_2$Ce(NO$_3$)$_6$ or CAN) as a chemical oxidant. In aqueous media, a solvent water molecule coordinates complex **WOC5**, generating the corresponding Ru–OH$_2$ complex with concomitant decoordination of one of the pyridyls of the equatorial 2,2′-bipyridine-6,6′-dicarboxylate ([bdc]$^{2-}$) ligand. When the Ru(IV) oxidation state is reached, the ruthenium metal centre can accommodate a seventh coordinated ligand, thus recovering the complete pyridyl coordination from the [bdc]$^{2-}$ ligand.[22] An additional oxidation step to Ru(V) and dimerization *via* a bimolecular I2M pathway, yields a Ru(IV)–O–O–Ru(IV) intermediate. The dimeric peroxo species can subsequently release molecular oxygen, however, under catalytic conditions in the presence of an excess of Ce(IV), the Ru(IV)–O–O–Ru(IV) intermediate is

further oxidised to Ru(IV)–O–O–Ru(V) or to its superoxide analogue, which can also release dioxygen.

Another remarkable example is a manganese complex (**WOC8**) capable of oxidising water to oxygen using a one electron donor type of oxidant, such as [Ru(bpy)$_3$]$^{3+}$. The performance of this catalyst has been tested at pH 7.2 (0.1 M phosphate buffer), yielding a TON of 25 with a TOF of 0.027 s^{-1}.[23]

A number of Ir complexes have also been proposed to work as WOCs, although it is not clear whether they are catalyst precursors to other molecular species that do the catalytic job or simply precursors to iridium oxide nanoparticles that are known to be active WOCs.[19]

3.3.2. Electrochemically induced WO. This activation strategy uses a potentiostat as the electron source, in order to apply the most appropriate potential at desired pH. Within electrochemically induced water oxidation, there are mainly two strategies that can be followed, depending on whether (i) the catalyst is in the homogeneous phase or (ii) is anchored onto the electrode surface. This second approach is a step further towards incorporating the WOC into a photoelectrochemical cell. Furthermore, this strategy can also enhance the reactivity, by stabilising the WOC after its heterogenisation. Different methods can be used to anchor a homogenous catalyst onto a surface: (i) physisorption, exploiting Van der Waals forces; (ii) electrostatic interaction, taking advantage of the different charges between the surface and the WOC; (iii) encapsulation, immobilizing the catalyst inside a matrix, and (iv) chemisorption, covalent bonding of the catalyst to the surface. In most of these examples, a previous modification of either the surface or the complex is needed.

Following the heterogenisation strategy, the best results belong to the mononuclear ruthenium catalyst (**WOC9**), covalently linked to a [Ru(bpy)$_3$]-type redox mediator. In this example, the catalyst is covalently anchored onto an ITO (Indium Tin Oxide) conducting glass through the interaction between the terminal

8 | Chem. Soc. Rev., 2014, 00, 1–19

This journal is © The Royal Society of Chemistry 2014

–OH surface groups and the phosphonate moieties. The new electrodes present the best performance reported until now towards water oxidation, with at least 2.8×10^4 TON and 0.6 s^{-1} TOF, applying 0.63 V overpotential at pH 1 and yielding a 97% faradic efficiency (*i.e.* 97% of the current is used to evolve oxygen).[24]

Recently, two different copper catalysts capable of oxidising water with a high faradic efficiency, high TOF, have been published. In the first example, the catalyst was a mononuclear compound (**WOC10**) capable of oxidising water by applying 0.75 V overpotential at pH 13, with a TOF of 100 s^{-1} and 90% faradic efficiency.[25] The second mononuclear copper compound (**WOC11**) oxidises water at 0.72 V overpotential at pH 11 with a comparable TOF and with 99% faradic efficiency. A water nucleophilic attack on the Cu(IV)=O or Cu(III)–O is proposed as the reaction mechanism.[26]

Another interesting example reports the WO by a molecular cobalt catalyst (**WOC4**), yielding 77% faradic efficiency, by applying 0.9 V overpotential (phosphate buffer, pH 2). The molecular nature of this catalyst has been proved by studying how the catalytic performance was affected by changing the ancillary ligands.[27] The mechanism has been proposed to be similar to the structurally related Ru **WOC3** and, similarly, involving the intramolecular interaction of the two Co(IV)=O units (I2M).

3.3.3. Photochemically induced WO. The use of sunlight to carry out water oxidation is one of the key points required to mimic the natural photosynthesis. Thus, the presence of a light harvesting system is fundamental in order to use sunlight energy to oxidise the WOC and to accumulate the oxidative equivalents needed to evolve oxygen.

As discussed previously in Section 2.4, light-induced water oxidation can be carried out in the homogenous phase using a photosensitiser (P) to harvest the sunlight energy, a WOC and a sacrificial electron acceptor (SEA) (Scheme 4). The absorption of sunlight energy by the photosensitiser generates an excited state (P*) capable of transferring an electron to the SEA and generating the oxidised photosensitiser (P$^+$). The latter then oxidises the WOC from its low oxidation state to a higher one, which in turn oxidises water to dioxygen.

Different WOCs have been tested in this three component system with moderate results.[2] One of the main problems of this approach is the photosensitiser stability, which can be oxidised by singlet oxygen generated during the catalysis from the direct interaction between the triplet oxygen and light.

One of the best results belongs to the three component system **WOC2**/**P3**/$Na_2S_2O_8$.[17] This example presents the maximum reported quantum yield ϕ_{O_2} (*i.e.* the number of photons used to generate oxygen), which turns out to be 0.3. Taking into account that for $Na_2S_2O_8$-based systems the maximum expected ϕ_{O_2} is 0.5, in the above-mentioned example 60% of the photons are used to generated oxygen. Furthermore, 90% of the $Na_2S_2O_8$ is consumed, which also turns to be one of the best reported results.

Another strategy for light-driven water oxidation is to build chromophore–catalyst dyad molecules. This approach consists
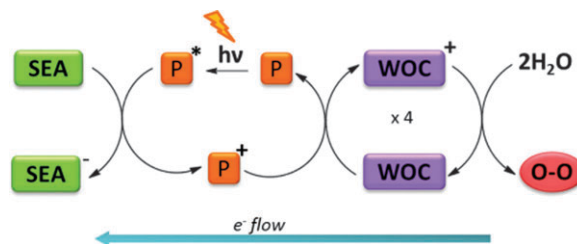
Scheme 4 Combination of reactions involved in light induced WO. WOC, catalyst in non-active oxidation state. WOC$^+$, catalyst in its active oxidation state. P, photosensitiser. SEA, sacrificial electron acceptor.

of covalently linking two metal complexes, each of them playing a different role: one acts as the light-harvesting antenna and the other one acts as the WOC. Most of the published dyads are used either to oxidise organic substrates or to study the electron transfer between the two metal centres. However, recently a diruthenium dyad (**D1** in Fig. 3) capable of reaching 134 TON upon light irradiation during 6 hours has been published. Moreover, the performance of this new dyad is better than the analogous three component system.[18]

Finally, anchoring the photosensitiser and the catalyst onto n-type semiconductor surfaces forms a photoanode, which can be incorporated in a PEC (see Section 6.2).

4. Proton reduction

4.1. Introduction

The reduction of protons into molecular hydrogen is a two-electron process (eqn (5) in Table 1), and from a thermodynamic point of view, all the redox couples with a more reductive potential than the couple $E(H_2O/H_2) = -0.41$ V *vs.* NHE at pH 7 are able to generate H_2. However, some of those reactions are kinetically disfavoured and are too slow in the absence of a suitable catalyst. Transition metal complexes can store electrons *via* multiple redox states and therefore they are suitable candidates to efficiently catalyse this reaction.[3,4,28,29] Indeed, during the last few decades a large number of homogeneous and heterogeneous molecular systems based on transition metal complexes for hydrogen evolution have been described. Even though they often show high efficiency and turnover numbers (TON) for hydrogen production, most of them are only functional in organic or aqueous-organic media (5–50% H_2O) and examples of systems working in pure water remain scarce. Nevertheless this is a necessary condition for a real application in a large scale artificial photosynthetic process.

In the following sections, an overview of the mechanistic proposal for proton reduction catalysed by metallic complexes will be presented, followed by a summary of the best molecular HECs described to date, selected according to their performance and focusing on those that work in aqueous conditions or hydro-organic media.

The HECs have been divided into two major categories, the first one includes catalysts based on rhodium and platinum, while the second one deals with those based on cobalt, nickel,

This journal is © The Royal Society of Chemistry 2014

Chem. Soc. Rev., 2014, **00**, 1–19 | 9
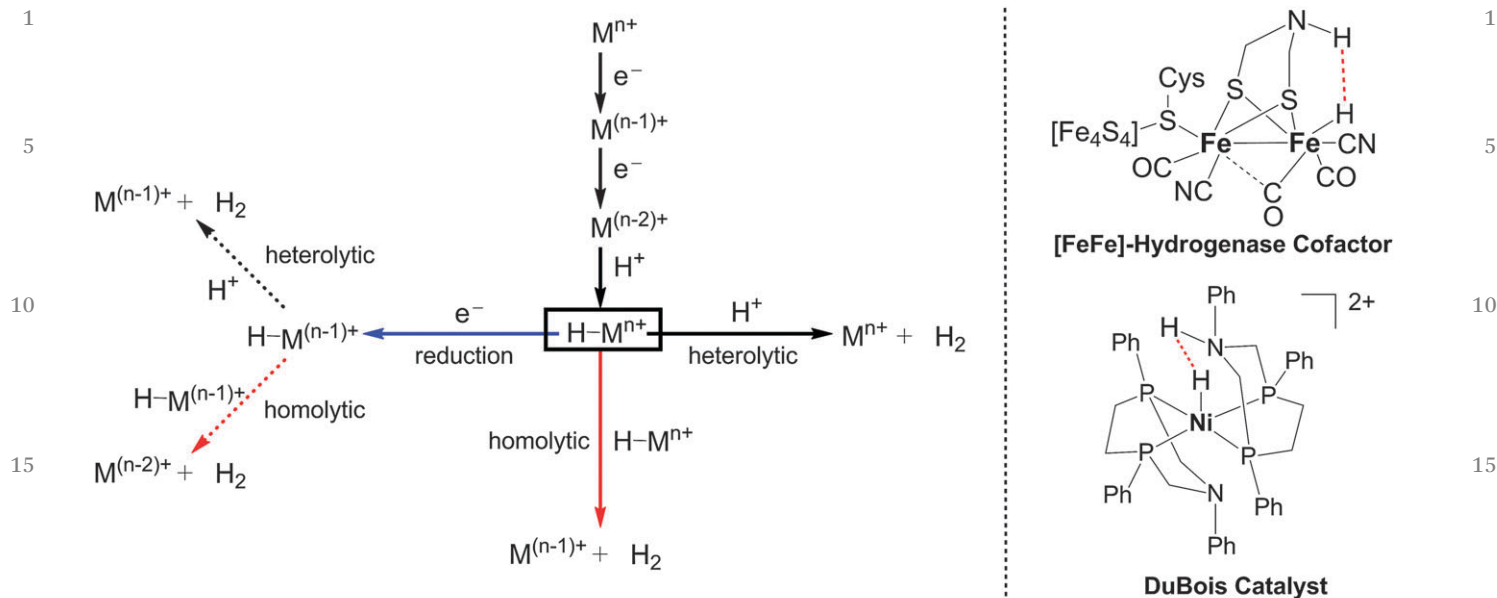
Scheme 5 Left, proposed mechanistic pathways for hydrogen evolution catalysis at a metallic centre M^{n+}. Right, hypothetical transition states of H–H bond formation at the [FeFe]-hydrogenase cofactor and DuBois catalyst.[31]

iron or molybdenum. The first family of metals has been studied for a long time because of their high reactivity towards protons as colloids and their ability to easily form metal hydrides. However their high costs and low abundances render them problematic for industrial applications. For this reason many new studies are focused on the development and the optimisation of metallic complexes based on cheaper and more abundant metals.

4.2. Proton reduction mechanisms

The mechanism of proton reduction catalysis at metallic centres has been studied experimentally and theoretically, particularly using cobalt, nickel and diiron catalysts.[3,4,28,30] Even though most of these studies have been done in organic media, they provide valuable information for the design of better catalysts that will ultimately be used under aqueous conditions.

A generic mechanistic scheme for proton reduction at a metallic centre M^{n+} is given in Scheme 5. Reduction of M^{n+} followed by protonation affords the key intermediate hydride $H–M^{n+}$ that can react in three different ways. The first one involves protonation and hydrogen evolution, regenerating the starting M^{n+} catalyst (heterolytic pathway, black arrow). Alternatively, the reaction with a second hydride molecule forms $M^{(n-1)+}$ and releases hydrogen (homolytic pathway, red arrow). The third possible route involves further reduction of the hydride to give a low valent hydride $H–M^{(n-1)+}$, which can analogously follow the heterolytic or homolytic pathways (blue arrow).

Homolytic and heterolytic pathways are competing mechanisms that can operate uniquely or simultaneously, depending on the experimental conditions, such as the catalyst concentration or pH. In this context, the use of bimetallic complexes can provide a useful tool to discriminate in favour of one mechanism and to enhance the rate of the catalysis.

The presence of proton relays in the second coordination sphere of the metal catalyst can favour Proton Coupled Electron Transfer (PCET) processes in hydrogen evolving catalysis. It has been proven that they facilitate the formation of the $H–M^{n+}$ hydride intermediate as well as the formation of the H–H bond. One illustrative example is that of DuBois catalysts in Scheme 5 with strategically positioned amine groups that are believed to be responsible for the high catalytic rates of the catalysis.[28,31] Very often this proton relay is compared to the cofactor of the [FeFe]-hydrogenase, the best natural enzyme for proton reduction and hydrogen oxidation (Scheme 5).

4.3. Catalysts

4.3.1. Pt and Rh. The first examples of functional photo-induced hydrogen production were published in the late seventies. They combine [Ru(bpy)$_3$]$^{2+}$ (**P2**) as a light harvester, a heterogeneous (platinum colloid) or homogenous (metal complex) proton reduction catalyst and a sacrificial electron donor (SED). Those systems can be coupled to a redox mediator such as methyl viologen (MV^{2+}) or metal complexes. In 1979 Lehn and Sauvage[3] showed that a **P2** photosensitized aqueous solution of colloidal platinum, using **HEC1** (Fig. 5) as electron relay, can efficiently evolve H$_2$ under visible light irradiation ($\lambda > 400$ nm, 10.8 h^{-1} TOF). They also showed that an equivalent solution at pH 5.2 without platinum colloids produced a significant amount of hydrogen (6 TON in 3 h); in this case the rhodium complex **HEC1** plays the role of hydrogen evolving catalyst in the first fully molecular photocatalytic system for proton reduction.

The most active rhodium catalyst (**HEC2**) belongs as well to the polypyridyl family and is able to reach more than 5000 TON with 34% of quantum yield (ϕ_{H_2}) in a system described by Bernhard.[3] Complex **HEC2** was coupled to a cyclometalated iridium photosensitiser (**P6**, Fig. 3) and TEA (triethylamine) was
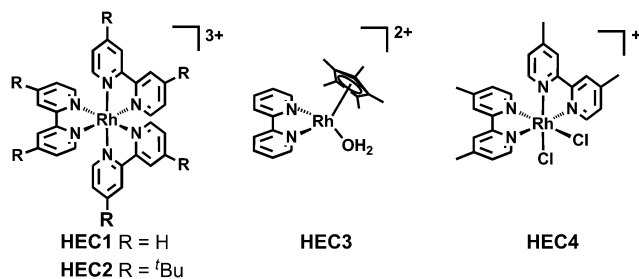
Fig. 5 A selection of rhodium hydrogen evolving catalysts.

used as the SED in an aqueous–organic solvent mixture THF : H_2O (80 : 20) under monochromatic irradiation (λ = 460 nm). An important drawback of this system is the presence of an organic co-solvent in addition to water.

In the last few years two new systems based on a rhodium catalyst that exhibit interesting activity in purely aqueous medium have been published. The first one was developed by Fukuzumi[32] and is built with pentamethylcyclopentadienyl and bipyridine ligands (**HEC3**, Fig. 5). This Rh catalyst was used together with **P2** as a photosensitiser and sodium ascorbate/ ascorbic acid buffer which acted as both the proton source and the electron donor. Under optimized conditions the catalyst can reach up to 100 TON in 3 h under visible light irradiation (λ > 430 nm). One interesting part of this work is the pH to reactivity relationship study. It has been shown that the optimal pH corresponds to a compromise between the reactivity of the catalyst towards protons and the efficiency of the quenching of the photosensitiser and therefore the sodium ascorbate/ascorbic acid ratio has to be chosen wisely to optimize the efficiency of the system. The second system is the most active rhodium based catalyst that works in purely aqueous medium and has been described by Collomb.[33] This system is composed of the poly-pyridyl catalyst **HEC4** in Fig. 5, which is similar to those used by Lehn and Bernhard, and uses **P2** as a photosensitiser and ascorbate buffer as an electron donor. The photocatalytic solution is irradiated under visible light (400 nm < λ < 700 nm) and under optimized conditions the system reaches more than 1000 TON. This work also highlights a non-negligible hydrogen production from a blank solution containing a mixture of the photosensitiser and the buffer at pH 4 that has to be taken into account, particularly when the catalyst concentration is lower than that of the photosensitiser.

The group of Sakai has developed numerous photocatalytic proton reduction systems that are active in pure water.[29] They are mainly based on platinum complexes (mono- and binuclear) with a nitrogen rich coordination sphere (Fig. 6).
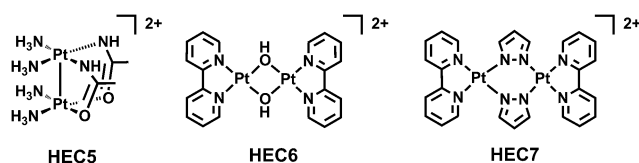
Fig. 6 A selection of binuclear platinum hydrogen evolving catalysts.

The best performances were obtained using the dinuclear complex **HEC5** (Fig. 6), **P2** as a photosensitiser, methyl viologen (MV^{2+}) as an electron mediator and EDTA (ethylenediamine tetraacetic acid) as an SED in acetate buffered aqueous solution (pH 5). In this case, the quantum yield (ϕ_{H_2}) for H_2 production can reach an exceptionally high value of 31% using visible light with an average TON around 100. According to the authors, the determining factors for the catalyst efficiency and activity are the distance and the interaction force between the d_{z^2} orbitals of the two platinum centres involved in the key hydride inter-mediate formation and thus in the proton activation process. The shorter the distance and/or the stronger the interaction between the two metal centres, the more active is the catalyst. To confirm this assertion, two other Pt dinuclear complexes with different Pt–Pt bond lengths were studied (**HEC6** and **HEC7**, Fig. 6). Indeed, complex **HEC6** with a shorter Pt–Pt bond length is more active than complex **HEC7** with a longer Pt–Pt bond. The overriding role of the platinum d_{z^2} orbitals in the proton reduction performance has also been confirmed for mononuclear platinum complexes by tuning their energy level using different coordination spheres and then studying the effects on proton reduction catalysis.[29]

4.3.2. Fe, Co, Ni and Mo. In the last 5–10 years there has been a remarkable improvement in the performance of water reduction catalysts using earth abundant materials like molybdenum or the first row transition metals iron, cobalt and nickel. Fig. 7 and 8 illustrate the best molecular catalysts described to date that belong to this group. The selection includes catalysts that have been used in aqueous media or those that have shown particularly interesting or exceptional properties in aqueous–organic solvents. Fig. 7 shows a collection of catalysts that have worked successfully under photochemical reactions, while Fig. 8 focuses on those that have only been used in electrocatalysis.

Since the cobaloxime-type complex $[Co(dmgH)_2]$ ($dmgH_2$ = dimethylglyoxime) was reported to promote photocatalytic proton reduction using **P2** as a photosensitiser, a large family of diimine/ dioxime cobalt HECs have been described.[3,28] They have shown high activity in organic media and have provided valuable insights into the proton reduction mechanism,[30] however, the low stability of this kind of complexes in water under acidic reductive conditions has limited their use in aqueous systems, particularly under homogeneous conditions. One example of a successful homogenous photocatalytic system in pure water uses complex **HEC8** in Fig. 7, together with natural photosystem I (PSI) as a photosensitiser and ascorbic acid as an SED.[3] The hetero-geneous approach, that is the use of catalysts attached on solid surfaces, has been proven to be a good strategy to improve the performance of cobaloxime type complexes.[4,28,34] Artero and coworkers fabricated a highly active cathode grafted with catalyst **HEC14** reaching up to 5.5×10^4 TON at −0.59 V vs. RHE (Fig. 8).[34] Electrodeposition of catalyst **HEC15** (Fig. 8, X = CH_3CN) on the glassy carbon electrode produced an electrocatalytic material that had 5×10^6 TON at −0.61 V vs. NHE.[4] It is worth noticing that in this kind of systems it is difficult to prove the molecular nature of the catalyst and formation of cobalt oxide nanoparticles cannot be ruled out.
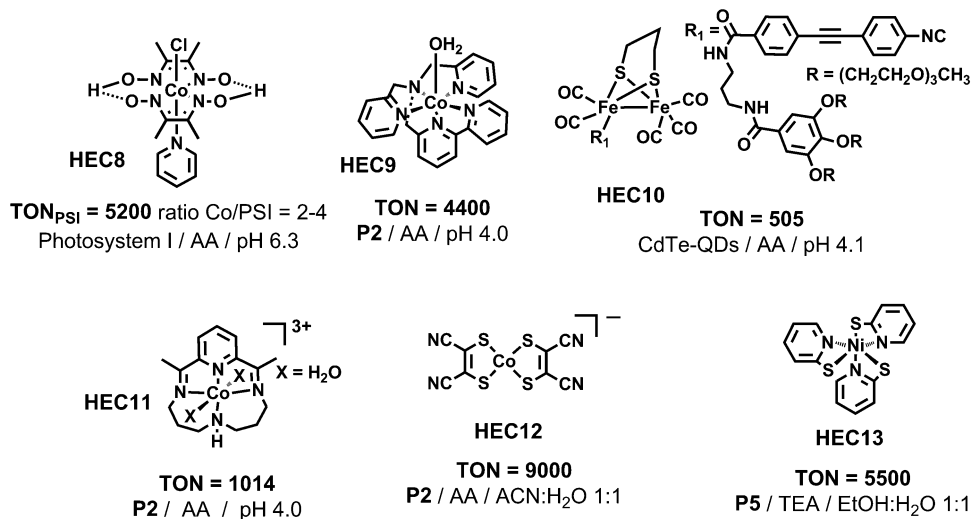
Fig. 7 A selection of hydrogen evolving photocatalysts containing Fe, Co or Ni, that work in aqueous media or aqueous–organic solvents. Turnover numbers (TON) are referred as moles of H_2 per mole of catalyst, unless otherwise indicated. Photosensitisers and sacrificial electron donors are added for comparison. AA = ascorbic acid/sodium ascorbate, TEA = triethylamine.
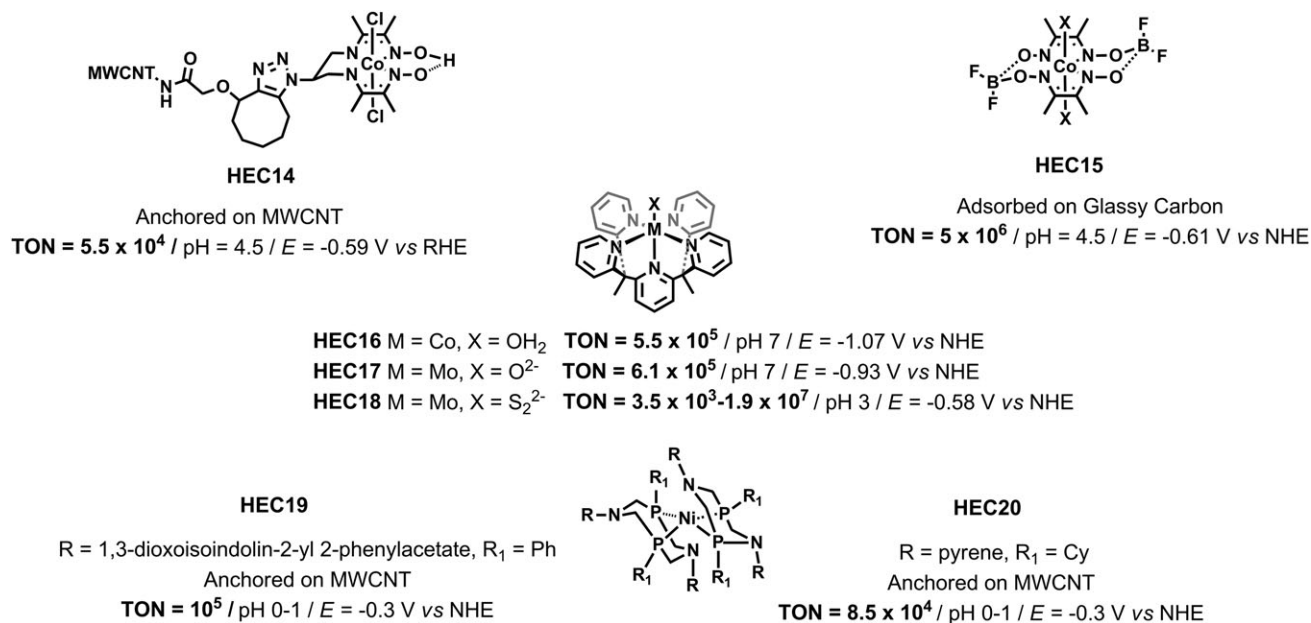
Fig. 8 A selection of hydrogen evolving electrocatalysts containing Co, Ni and Mo which work in aqueous media. Turnover numbers (TON) are referred as moles of H_2 per mole of catalyst.

On the other hand, cobalt complexes stabilized by other nitrogen donor ligands have shown remarkable stability in water and high activity in both photochemical and electrochemical systems as illustrated by the selected examples **HEC9**, **HEC11** and **HEC16** in Fig. 6 and 7.[3,4,35] Polypyridyl-based ligands have also been used to prepare high-valent molybdenum catalysts **HEC17** and **HEC18** in Fig. 8, which are among the best molecular electrocatalysts for hydrogen production described to date that perform in pure water. Complex **HEC18** (3.5×10^3 to 1.9×10^7 TON) is considered a molecular analogue of the edge sites of two-dimensional bulk MoS_2, that has also been used in water reduction.[4]

Iron based catalysts have also been extensively studied as HEC. Most of them are dimeric iron(I) complexes resembling the natural enzyme [FeFe]-hydrogenase cofactor. A problem associated with these mimics is the low solubility in water but this can be solved by encapsulating the catalyst inside micelles or cyclodextrins, attaching the catalyst on a solid support or by using ligands with water affinity.[3,28] One example of this latter strategy is described in recent work by Wu where they use a ligand containing trimeric ethylene glycol chains (see **HEC10** in Fig. 7). They achieve 505 TON under visible light irradiation using CdTe nanocrystals as photosensitisers and ascorbic acid as an SED under pure aqueous conditions.[3]

12 | *Chem. Soc. Rev.*, 2014, **00**, 1–19

This journal is © The Royal Society of Chemistry 2014

Diphosphine nickel complexes of the type of **HEC19** and **HEC20** in Fig. 8 were first developed by DuBois and coworkers as HECs in organic solvents but not in water due to their limited solubility.[3,4,28,31] Two independent studies by Artero and coworkers were published later where they attached catalysts **HEC19** and **HEC20** to MWCNTs (multiwalled carbon nanotubes) by covalent bonding or pi-stacking interactions, respectively. Subsequent dropcasting on glassy carbon using Nafion afforded electrocatalytically active electrodes achieving up to 8.5×10^4 TON in pure aqueous systems.

Another emerging group of HEC studied by Eisenberg are those based on sulfur donor ligands, which are usually redox non-innocent and are thought to have a role in the mechanism of proton reduction. We find examples of cobalt and nickel complexes in this group, **HEC12–13**, with both metals showing excellent photocatalytic activity in conjunction with **P2** or fluorescein (**P5**) photosensitisers.[3,4] All the examples of this family reported to date are described in aqueous–organic solvents.

5. CO$_2$ reduction

5.1. Introduction

Carbon dioxide is one of the major contributors to the greenhouse effect resulting in serious global warming, with the main source of this anthropogenic CO_2 being the burning of hydrocarbon fuels. However, CO_2 represents an important non-toxic, highly abundant and cheap carbon feedstock and should not be viewed as a waste material. In particular, the transformations of carbon dioxide into methanol or formic acid are important because these chemicals could be used as liquid fuels. Unfortunately, the inherent structural stability of the CO_2 molecule makes its activation towards reduction a difficult task. Therefore, among the contemporary energy challenges present today, the reduction of carbon dioxide is certainly one of the major issues.

Another complicated issue associated with the reduction of CO_2 is the fact that it can produce a variety of products such as formic acid, carbon monoxide, oxalic acid, methanol or methane

(see Table 1 in Section 1). As depicted in eqn (6), the injection of one electron into CO_2 requires a lot of energy; the potential of the $CO_2/CO_2^{\bullet-}$ redox couple is highly negative (-1.9 V vs. NHE). This high energy value is partly due to the rearrangement from a linear to a bent structure. On the other hand, proton-coupled multielectron transfer (PCET) processes are generally more favourable than single electron reductions because thermodynamically more stable molecules are produced and high energy barriers are avoided. This phenomenon is illustrated by the equations summarized in the Table 1 (compare reduction potential of eqn (1) with those of eqn (2)–(12)).

There are different methods to reduce CO_2 including electrocatalysis, photocatalysis or the use of chemical reducing agents such as hydrogen. Regardless of the employed methodology, the use of a catalyst is always required in order to avoid the formation of the CO_2 radical anion intermediate and to minimize the overpotential for the overall process. Molecular catalysts containing transition metals have been extensively used because low oxidation state species can easily be reached. However, most electrochemical and photochemical systems for CO_2 reduction only produce the $2e^-$ reduction products, that is, carbon monoxide or formate. One of the main challenges in this field is therefore to convert carbon dioxide to a more reduced product such as methanol with high efficiency and selectivity. The new catalysts for CO_2 reduction should also be highly sensitive to the gas in order to react at low concentration of CO_2, ideally at atmospheric concentrations.

In the following section, an overview of the mechanistic proposal for carbon dioxide reduction catalysed by metallic complexes will be presented. Section 5.3 will then describe the best catalytic systems for CO_2 reduction based on complexes depicted in Fig. 9 where they have been divided into: (i) CO_2 reduction using H$_2$, (ii) electrocatalysis and (iii) photocatalysis.

5.2. Mechanisms

The first steps towards CO_2 reduction is its coordination to a reduced metallic centre (M^{n+}) to give $M^{n+}L(CO_2)$ (solid black arrows, Scheme 6). The CO_2 molecule possesses both acidic and
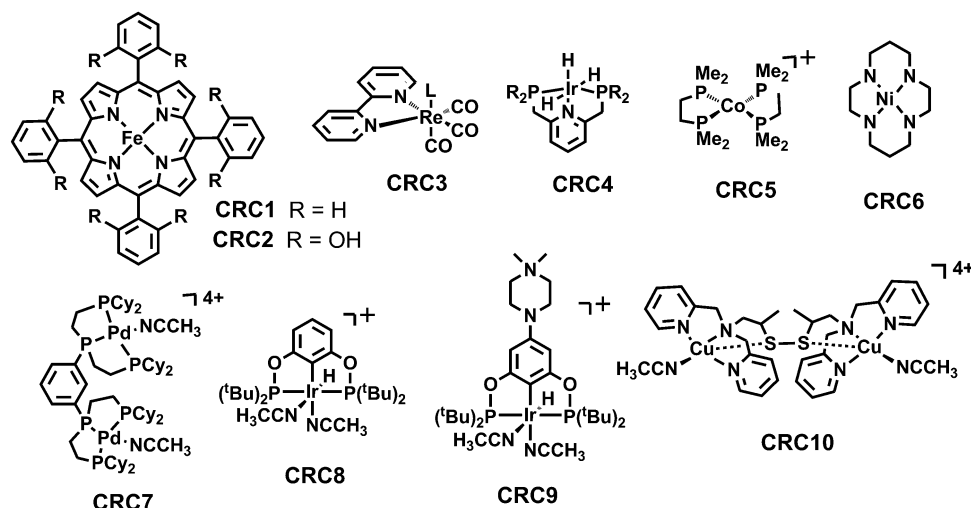
Fig. 9 A selection of carbon dioxide reduction catalysts.

CO bond cleavage

$$M^{n+}L \xrightarrow{e^-} M^{(n-1)+}L \xrightarrow{e^-} M^{(n-2)+}L \xrightarrow{CO_2} M^{m+}L(CO_2) \cdots\cdots\rightarrow M^{n+}L + CO + "O^{2-}"$$

$$\downarrow H^+$$

$$M^{n+}L + H_2 \xleftarrow{H^+} H-M^{n+}L \xrightarrow{CO_2} M^{m+}L(OCHO) \cdots\cdots\rightarrow M^{n+}L + HCO_2^-$$

$$M \xrightarrow{H_2} M\overset{H}{\underset{H}{\langle}} \xrightarrow{B} \left[M \overset{H\cdots B}{\underset{H}{\langle}} \right] \xrightarrow{HB} M-H$$
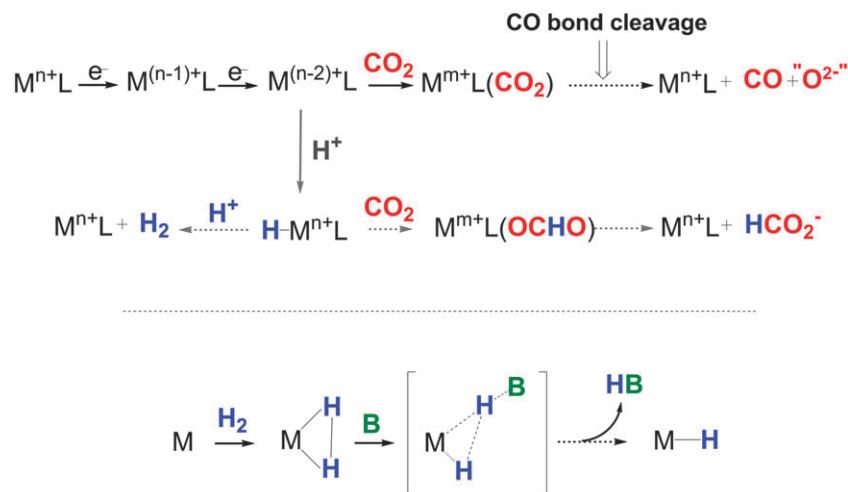
Scheme 6 Top, general scheme for the two electron CO_2 reduction catalysed by a metallic centre (M^{n+}). n^+, initial oxidation state of the CRC; m^+, intermediate oxidation state during catalysis turnover. Bottom, mechanism for the heterolytic cleavage of dihydrogen.

basic properties and the carbon atom is susceptible to be attacked by nucleophiles and the oxygen atoms are susceptible to be attacked by electrophiles. The most usual coordination modes of CO_2 to a transition metal centre are the σ-bonding of the metal to the electrophilic carbon atom. During catalyst turnover, a competition may occur between the addition of CO_2 and addition of H^+ on the active reduced form of the catalyst leading to bond cleavage and release of CO (black dashed arrow) or to a metal hydride intermediate H–M^{n+}L (solid grey arrow). This metal hydride can undergo two competing processes; it can either react with CO_2 to give the desired formate (HCO_2^-) or it can react with H^+ to produce molecular hydrogen (H_2) (compare left and right dashed grey lines). The acidity of the reaction medium may influence the product distribution between CO, formate and H_2.

The reduction of CO_2 to CO requires the cleavage of a C–O bond (black dashed arrow in Scheme 6). A detailed kinetic analysis of the catalytic reduction of CO_2 to CO by an electro-generated iron(0) porphyrin derived from **CRC1** in Fig. 9, in the presence of a Brønsted acid has recently been described.[36] By means of a systematic application of the foot of the wave strategy to cyclic voltammetric responses, it is found that the rate-determining step is a reaction in which electron transfer from the central iron atom is concerted with proton transfer and breaking of one C–O bond. This was the first time that such a concerted proton–electron transfer bond cleavage was detected and characterised in a catalytic process. Experimental and theoretical studies of the role of weak Brønsted acids were also performed on the catalysis of the reduction of CO_2 to CO using a rhenium catalyst of the type of **CRC3** (L = Cl).[37,38] Here it was shown that addition of a proton source speeds up the catalysis considerably.

The mechanism of the photocatalytic reduction of CO_2 has been extensively studied using $[Re^I(bpy)(CO)_3L]$ (**CRC3**) based complexes. After photoexcitation, the next step is the reductive quenching of the MLCT (Metal to Ligand Charge Transfer) excited state of the rhenium complex by a sacrificial electron

donor (SED) yielding the one-electron reduced species $[Re^I(bpy^\bullet)(CO)_3L]^-$. It is proposed that the following step is a ligand exchange with the solvent to afford the catalytically active species, however, the mechanism of CO formation is still not completely elucidated. In some cases a CO_2^- or C(OH)O-bridged dinuclear species was observed or isolated.

Three different processes for the reduction of CO_2 in the presence of hydrogen are generally identified: (i) hydride formation, (ii) hydride transfer from the metal complex to the coordinated CO_2 and (iii) H_2 coordination concomitant with transformed-substrate release. The key mechanistic step is the heterolytic activation of dihydrogen by the transition metal complexes (Scheme 6, bottom). The heterolytic cleavage of the H_2 ligand is triggered by a base which can be an external base or an intramolecular ancillary ligand, yielding the metal hydride intermediate species (black dotted arrow in Scheme 6, bottom). The hydride transfer step appears to be similar to those observed in the photo- and electrocatalysis (grey dotted arrows in Scheme 6, top).

5.3. Catalysis

5.3.1. CO_2 reduction with H_2. The reduction of CO_2 using transition metal catalysts and molecular hydrogen as the reducing agent is a useful methodology to transform CO_2 into C_1 products such as formic acid, formaldehyde, methanol and methane. Different kinds of molecular catalysts have been studied for CO_2 reduction under a hydrogen atmosphere; the most efficient ones are based on noble metals such as iridium, ruthenium or rhodium.[39]

One of the most active catalysts described to date for the reduction of CO_2 with hydrogen is the iridium pincer complex **CRC4** in Fig. 9,[39] that performed 3.5×10^6 TON with a TOF up to 40 s^{-1} ($T = 200$ °C, $P_{H_2} = 25$ atm, $P_{CO_2} = 25$ atm).

An important challenge still remaining in this field is the design of catalysts that are highly sensitive to CO_2, that is to say, catalysts that react with atmospheric concentration of CO_2 (390 ppm) or lower. In this context, Linehan has recently developed a system based on a first row transition metal.[40]

14 | *Chem. Soc. Rev.*, 2014, **00**, 1–19

This journal is © The Royal Society of Chemistry 2014

The cobalt hydride derived from **CRC5** produces formate from CO_2 and H_2. This complex presents a high catalytic activity with a TOF of 3400 h^{-1} at room temperature and using a mixture of gases of $CO_2 : H_2$ (1 : 1) at P = 1 atm. The catalytic activity is comparable to those of noble metal catalysts for CO_2 reduction with hydrogen, however, this catalytic system requires the use of a quite exotic/expensive base.

5.3.2. Electrocatalytic reduction of CO_2. The electrocatalytic reduction of CO_2 can yield different products depending on the degree of reduction that is achieved after catalysis (eqn (6)–(12), Table 1). To facilitate the discussion of this topic, this section has been divided into three categories according to the product that is generated after reduction, *i.e.* (i) carbon monoxide, (ii) formate, (iii) oxalate.

(i) Reduction to CO: A plethora of organometallic complexes have been studied as catalysts for the CO_2 activation and its electrochemical conversion to CO (eqn (8), Table 1).[5] Among them, iron porphyrins have shown remarkable results. For instance, Saveant and coworkers reported catalyst **CRC1** in Fig. 9 as an efficient and stable catalyst for the selective conversion of CO_2 into CO in the presence of Lewis acids or weak Brønsted acids.[5] In this work, it was also observed that the addition of a proton source speeds up the catalysis. On this basis, the same group reported catalyst **CRC2, shown** in Fig. 9, bearing hydroxyl groups on the phenyl group perpendicular to the macrocycle of the porphyrin, leading to a considerable increase of catalytic activity.[5] This catalyst, which uses one of the most earth abundant metals, presents good selectivity towards the production of CO (above 90%) with a TON of 5×10^7. Furthermore, the catalyst remains stable over the course of 4 hours of electrolysis at a low overpotential (0.465 V).

Catalysts based on other macrocyclic structures have also been studied.[41] In 1980, Eisenberg reported a family of tetra-azomacrocyclic complexes of cobalt and nickel similar to **CRC6** shown in Fig. 9 for the reduction of CO_2 to CO. These catalysts performed with high current efficiencies (up to 98%) and at potentials ranging from -1.3 to -1.6 V *vs.* SCE (E(V) *vs.* SCE = E(V) *vs.* NHE -0.2412 V).[41] A few years later, the group of Sauvage reported the nickel cyclam complex **CRC6**.[41] This complex was extremely stable and displayed good selectivity and faradic efficiency (up to 96%) at -0.86 V *vs.* SCE (E(V) *vs.* SCE = E(V) *vs.* NHE -0.2412 V) in aqueous solution. However, it has been shown that Ni(cyclam) complexes are absorbed on the mercury electrode. More recently the homogeneous CO_2 reduction activity of this catalyst was examined at a glassy carbon electrode,[42] and it was shown that even if the same catalyst presents a better activity on mercury, the catalysis occurs efficiently and selectively in water also on an inert electrode. Another family of metal catalysts used for the reduction of CO_2 to CO are those containing phosphine ligands such as the bimetallic palladium complex **CRC7**, shown in Fig. 9, studied by DuBois. This complex shows high catalytic rate and faradic efficiencies higher than 90% for CO production in acidic acetonitrile solution. They suggest cooperative binding of CO_2 that facilitates the formation of the CO_2 adduct intermediate.[5]

(ii) Reduction to formate: Formic acid is one of the two possible $2e^-$ reduction products of CO_2 (eqn (7), Table 1). It is the only product of the electrolysis of CO_2 in water on an inert electrode without any catalyst present. The transformation of CO_2 into formate is an interesting option because formic acid may be used for hydrogen storage, as a reducing agent for organic compounds or as a liquid fuel in formic acid fuel cell applications.

Iridium pincer complexes such as **CRC8** and **CRC9** have been developed to electrochemically reduce CO_2 to formate in a mixture of water–acetonitrile or in pure water, respectively.[43] Both electrocatalysts are highly active for the CO_2 reduction with faradic yields up to 90% and formate being the only reduced carbon product of the reaction. However, simultaneous production of H_2 from the reduction of water was also observed.

(iii) Reduction to oxalate: Oxalate is one of the products of the direct reduction of CO_2 on an inert electrode in aprotic media, together with carbon monoxide. It generates from the dimerization of the initial CO_2 anion radical (eqn (6) and (9), Table 1), however, a high overpotential is required to perform this reaction and therefore the use of a catalyst is highly desirable.

A remarkable catalytic system that has been developed in this context is the dinuclear copper complex **CRC10** shown in Fig. 9 and Scheme 7.[5] The two electron reduced complex derived from **CRC10** reacts selectively with CO_2 from air rather than O_2 to generate a tetranuclear complex containing two bridging CO_2-derived oxalate groups (steps a–c in Scheme 7). Addition of a lithium salt to the copper(ii) oxalate complex results in quantitative precipitation of lithium oxalate (step d in Scheme 7). This catalytic system is able to activate and transform CO_2 selectively into oxalate by applying -0.03 V *vs.* NHE.

5.3.3. Photoactivated CO_2 reduction. Photocatalytic reduction of CO_2 using solar energy is another attractive option to activate CO_2, especially in terms of sustainability since the energy needed to run the reaction comes from sunlight.[44] The first example of photocatalytic CO_2 reduction was published by Lehn in the early eighties.[41] They used $[Ru(bpy)_3]^{2+}$ (**P2**) as a photosensitizer, $CoCl_2$ as a catalyst, and TEOA (triethanolamine) as a sacrificial electron donor (SED) in aqueous solution. This system displays a quantum yield (ϕ_{CO}) of 0.012. The same group presented the photocatalyst $[Re(bpy)(CO)_3Cl]$ (**CRC3**) with a ϕ_{CO} = 0.14 and good selectivity.[41] The rhenium complex plays a double role in the reaction because it both absorbs the light and performs the catalytic CO_2 reduction. One of the main drawbacks of the latter system is that the complex absorbs mostly in the UV light region, with weak absorption in the visible part of the solar spectrum. In order to overcome this problem, the catalyst is covalently linked to a visible light absorbing photosensitizer in the form a dyad, such as in **D3** in Fig. 3. This photocatalyst was developed by Ishitani and coworkers and displayed high selectivity for the CO generation with ϕ_{CO} = 0.12 and 170 TON under visible light irradiation.[44]

The same group has developed supramolecular photocatalysts with different ratios of photosensitiser units and catalyst units based on ruthenium complexes.[45] These multinuclear

This journal is © The Royal Society of Chemistry 2014

Chem. Soc. Rev., 2014, **00**, 1–19 | **15**
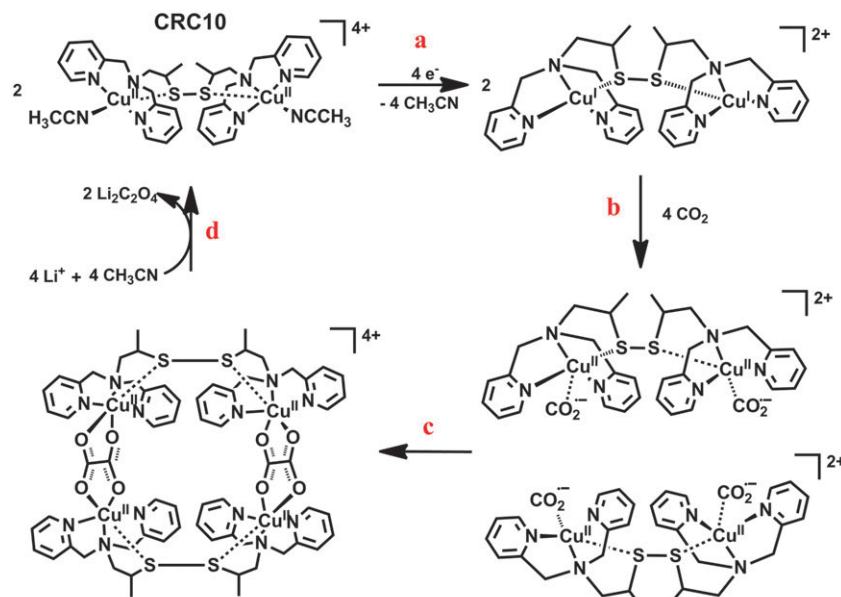
Scheme 7 Electrocatalytic reduction of CO_2 to oxalate catalyzed by **CRC10**.
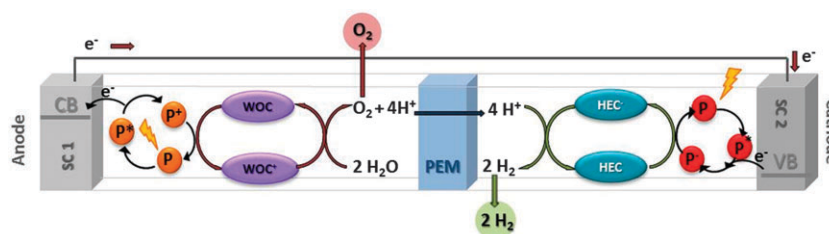
Fig. 10 Schematic representation of a photoelectrochemical cell (PEC) performing the overall light induced water splitting.

complexes were used as photocatalysts for the reduction of CO_2 to formic acid. In the case of the higher ratios of the photosensitiser unit **D4** shown in Fig. 3, they observed a high yield of formic acid and the highest photocatalytic activity with ϕ_{HCOOH} = 0.061 and 671 TON.

6. Photoelectrochemical cells (PECs)

6.1. Introduction

The conversion of solar energy into chemical fuels can be achieved *via* so-called water splitting, by means of sunlight-storing devices. The requirement to build such devices include the assembly of suitable modules for light harvesting, water oxidation and proton reduction in a single photoelectrochemical cell (PEC), mimicking natural photosynthesis.

The overall water splitting process can be divided into the two half reactions, so that water oxidation and proton reduction are carried out in two separate compartments. Each compartment contains an electrode (respectively the anode, performing water oxidation, and the cathode, performing proton reduction), connected through an external circuit for electron flow (see Fig. 10). At least one of the electrodes is coupled

to light absorption, *i.e.* it is photoactive. In this case, the role of a visible light harvester is usually played by the semiconducting material constituting the anode and/or the cathode. Depending on the energy band gap, the semiconductor itself can absorb the visible light or must be sensitised with a suitable dye molecule P (see Fig. 10 and Section 2.2). Furthermore, the anodic and cathodic compartments can host the water oxidation and the proton reduction catalysts respectively. The WOC and HEC can be molecular catalysts dissolved in the homogeneous phase (as shown in Fig. 10), but a PEC could also be designed so that one or both catalysts are anchored onto the electrode/photoelectrode. Finally, a proton exchange membrane (PEM) can be used to physically separate the two compartments, thus simplifying the product (O_2 and H_2) collection and avoiding their potentially hazardous reaction back to H_2O.

A common strategy to build PECs consists of optimising the properties of the half reactions independently. In this case, a simple metallic wire or mesh (*e.g.* platinum) can be used as the counter electrode, and a potentiostat is then used to apply the desired potential to probe the system. Once independently optimised, the modules should be conveniently integrated into the final device, ensuring the matching of both the current and

16 | *Chem. Soc. Rev.,* 2014, **00**, 1–19

This journal is © The Royal Society of Chemistry 2014
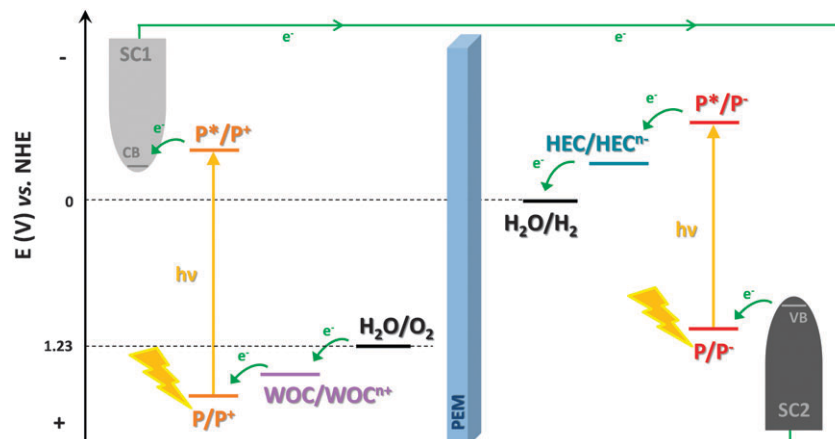
Fig. 11 Schematic representation of the thermodynamics occurring respectively at the photoanode (left) and the photocathode (right) of a PEC performing the overall light induced water splitting.

the potential of all the reactions involved in the whole process, in order to achieve high conversion efficiencies. For a schematic representation of the thermodynamics involved in the light assisted water splitting in a PEC see Fig. 11.

6.2. Molecular photoanodes for water oxidation

Focussing on the WO half-reaction, as previously indicated, a straightforward strategy is to integrate both the light absorbing molecule (P) and the water oxidation catalyst (WOC) on the surface of a n-type semiconductor, such as TiO_2 (SC1 in Fig. 10), thus yielding a single hybrid material that can potentially act as a photoanode. Aside from the WOC, that must be firmly anchored without modifying its intrinsic coordination and catalytic properties, an appropriate choice of the dye is also fundamental. The latter should display: (i) extended absorption in the visible spectrum; (ii) an oxidised state able to undergo fast photo-induced electron transfer with the WOC; and (iii) a suitable oxidation potential to drive the consecutive redox processes on the catalyst (see also Fig. 11).

Mallouk and coworkers reported the first example based on this strategy, where IrO_2 nanoparticles were organized onto dye-sensitized TiO_2.[46] Photocurrents up to 30 μA were registered when applying 0 mV vs. Ag/AgCl (E(V) vs. Ag/AgCl = E(V) vs. NHE −0.2881 V) bias and irradiating with a 450 nm light source in 30 mM $NaHCO_3$/Na_2SiF_6 buffer (pH 5.75). The formation of O_2 and H_2 at the two compartments of the PEC (separated by a glass frit) was confirmed by means of gas chromatography and Clark electrode measurements, yielding a faradic efficiency for O_2 generation of ca. 20%.[46]

After this pioneering example, several other PECs containing transition metal oxides as WOCs have been reported. On the other hand, assemblies involving molecular catalysts are still rare. The first example of a molecular catalyst anchored onto a photoanode was reported by Sun and coworkers.[47] The ruthenium complex WOC6 (Fig. 4) was confined in Nafion, and deposited onto a dye-sensitised TiO_2 electrode. Visible light-driven water splitting was successfully achieved upon both illumination (provided by a light emitting diode of 100 mW cm^{-2}) and application of a −0.325 V vs. Ag/AgCl (E(V) vs. Ag/AgCl = E(V) vs. NHE −0.2881 V) bias to the device. Under these conditions, a photocurrent density of 43 μA cm^{-2} was obtained in 0.1 M Na_2SO_4 aqueous solution, although just a qualitative analysis of the generated hydrogen has been reported.

This system has been recently modified by the same group by covalently anchoring the catalyst (functionalized with a silane moiety, compound WOC7 in Fig. 4) onto the dye-sensitised TiO_2 surface.[48] By applying an external bias of 0.2 V vs. NHE, an initial photocurrent density of 1.7 mA cm^{-2} was registered upon illumination with a white light source of 300 mW cm^{-2} in phosphate buffer (pH 6.8). The production of both O_2 and H_2 during the water splitting process has been confirmed by means of gas chromatography. After 500 s of visible light illumination, ca. 0.75 μmol of O_2 and 1.34 μmol of H_2 were detected, corresponding to faradic efficiencies of 83% and 74% respectively.

6.3. Molecular photocathodes for proton reduction

With regard to the other half-reaction, proton reduction can be performed at a photocathode assembled from a p-type semiconductor electrode (SC2 in Fig. 10), eventually sensitised with a P and coupled with a HEC. The latter can be either in the homogeneous phase or anchored onto the semiconductor surface. The redox properties of both the dye and the catalyst must accomplish the requirements schematically shown in Fig. 11.

Recently some molecular photocathodes, coupled with platinum as the counter electrode, have been developed. For example, Sun and coworkers reported the covalent anchoring of the organic dye P7 onto a nanostructured p-type semiconductor (NiO, SC2 in Fig. 10).[49] The resulting photocathode was coupled with the cobalt complex HEC15 (X = H_2O) and used in phosphate buffer at pH 7. Initial photocurrents of ca. 5 μA cm^{-2} were generated by applying −0.4 V vs. Ag/AgCl bias (E(V) vs. Ag/AgCl = E(V) vs. NHE −0.2881 V) and illuminating with a light emitting diode. Hydrogen generation (ca. 90 nmol mL^{-1} after 30 min of irradiation) was confirmed using a modified Clark-type electrode.

This journal is © The Royal Society of Chemistry 2014

Chem. Soc. Rev., 2014, 00, 1–19 | 17

Another interesting example of a NiO-based photocathode was reported by Wu and coworkers.[50] In this system, the major improvements are related to both: (i) the coating of the NiO surface with an insulating monolayer of alumina (in order to suppress hole–electron recombination across the semiconductor surface) and (ii) the covalent anchoring of the HEC, in the form of the supramolecular dyad **D2** (Fig. 3). Upon irradiating this photocathode with a Xe lamp and applying 0.1 V vs. NHE bias to it, photocurrent densities up to 9 μA cm^{-2} were registered in both neutral water and phosphate buffer at pH 7. Hydrogen production (0.29 μmol) was confirmed by means of gas chromatography (calculated faradic yield = 45%).

Recently, Mozer and coworkers reported a molecular dye-sensitised photocathode coupled to a BiVO$_4$ photoanode, in a Pt-free tandem PEC performing the overall water splitting. In this device, a NiO photocathode, sensitised with **P8** (Fig. 3) was connected in series, side by side, to a BiVO$_4$ photoanode.[6] The two compartments of the PEC were separated by a Nafion PEM and the two photoelectrodes were illuminated simultaneously with visible light. The resulting PEC is a standalone system, i.e. able to sustain solar hydrogen generation without the application of an external electrical bias or the addition of a sacrificial oxidant/reductant. In 0.1 M Na$_2$SO$_4$ (pH 7), a steady photocurrent of 2.7 μA cm^{-2} was sustained over 4 hours. Hydrogen production (2.6 nmol) was confirmed by gas chromatography (97% faradic efficiency), whereas O$_2$ could not be detected.

6.4. PECs combining photocathodes for CO$_2$ reduction with O$_2$ evolving photoanodes

The same concept of using sunlight to split water and generate H$_2$ and O$_2$ can also be applied to water splitting assisted by CO$_2$ to generate O$_2$ and HCOOH (or other CO$_2$ reduction products), which is a close mimic of natural photosynthesis (eqn (17) and (18) respectively).

$$2CO_2 + 2H_2O \rightarrow 2HCOOH + O_2 \qquad (17)$$

$$nCO_2 + nH_2O \rightarrow (CH_2O)_n + nO_2 \qquad (18)$$
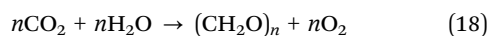
Photocatalytic CO$_2$ reduction yielding useful chemicals is a more challenging reaction than H$_2$ production and, when performed in aqueous solutions, suffers from both low product selectivity and low quantum efficiencies, due to competition with H$_2$ evolution. However, some interesting examples of these different kinds of PECs have been reported by Sato and coworkers.[44] The reduction of CO$_2$ to formate was catalysed by a ruthenium complex anchored onto different p-type semiconductors by means of polypyrrole polymerization. The most promising results were obtained by coupling a reduced SrTiO$_3$ photoanode with a zinc-doped indium phosphide (InP) photocathode (modified with the above mentioned catalyst) in a "wireless" fashion with no external bias. With this assembly, solar CO$_2$ reduction was successfully performed in a 0.1 M NaHCO$_3$ aqueous solution mixed with phosphoric acid (pH 7.7), with a conversion efficiency from solar to chemical energy of 0.08%.[7]

7. Final remarks

During the last decade the field has advanced enormously at all fronts and even though catalysts and photosensitizers should be further improved in terms of overall performance in aqueous solutions, the bases for the construction of a device are already set up. Today the main challenge ahead, for the construction of technologically useful PEC for the production of solar fuels, is the harmonization of all the numerous reactions that occur in each compartment. In other words, assuming that the thermodynamics of the whole PEC cell are correct, an indispensable requirement is that the kinetics of all the reactions involved are right so that the desired reactions occur. Given the combination of the large number of reactions involved this is by no means trivial.

Thus an enormous effort should be dedicated to the construction of complete PEC in order to fully understand the different parameters involved so that they can be adequately tuned for success.

The potential solution to today's energy problem has strong societal implication since it will allow us to maintain the lifestyle of our developed societies, and also to attain decent living standards in developing and poor countries.

Acknowledgements

References

1 N. S. Lewis and D. G. Nocera, *Proc. Natl. Acad. Sci. U. S. A.*, 2006, **103**, 15729–15735.

2 R. Bofill, J. García-Antón, L. Escriche, X. Sala and A. Llobet, in *Comprehensive Inorganic Chemistry II*, ed. J. Reedijk and K. Poeppelmeier, Elsevier, Amsterdam, 2nd edn, 2013, pp. 505–523.

3 W. T. Eckenhoff and R. Eisenberg, *Dalton Trans.*, 2012, **41**, 13004–13021.

4 V. S. Thoi, Y. Sun, J. R. Long and C. J. Chang, *Chem. Soc. Rev.*, 2013, **42**, 2388–2400.

5 C. Costentin, M. Robert and J. M. Saveant, *Chem. Soc. Rev.*, 2013, **42**, 2423–2436.

6 L. Tong, A. Iwase, A. Nattestad, U. Bach, M. Weidelener, G. Gotz, A. Mishra, P. Bauerle, R. Amal, G. G. Wallace and A. J. Mozer, *Energy Environ. Sci.*, 2012, **5**, 9472–9475.

7 T. Arai, S. Sato, T. Kajino and T. Morikawa, *Energy Environ. Sci.*, 2013, **6**, 1274–1282.

8 R. R. King, D. C. Law, K. M. Edmondson, C. M. Fetzer, G. S. Kinsey, H. Yoon, R. A. Sherif and N. H. Karam, *Appl. Phys. Lett.*, 2007, **90**, 183516.

9 K. Branker, M. J. M. Pathak and J. M. Pearce, *Renewable Sustainable Energy Rev.*, 2011, **15**, 4470–4482.

18 | *Chem. Soc. Rev.*, 2014, **00**, 1–19

This journal is © The Royal Society of Chemistry 2014

10 H. K. Jun, M. A. Careem and A. K. Arof, *Renewable Sustainable Energy Rev.*, 2013, **22**, 148–167.

11 A. Hagfeldt, G. Boschloo, L. Sun, L. Kloo and H. Pettersson, *Chem. Rev.*, 2010, **110**, 6595–6663.

12 B. O'Regan and M. Gratzel, *Nature*, 1991, **353**, 737–740.

13 J. Burschka, N. Pellet, S.-J. Moon, R. Humphry-Baker, P. Gao, M. K. Nazeeruddin and M. Gratzel, *Nature*, 2013, **499**, 316–319.

14 A. Fujishima and K. Honda, *Nature*, 1972, **238**, 37–38.

15 M. J. Katz, S. C. Riha, N. C. Jeong, A. B. F. Martinson, O. K. Farha and J. T. Hupp, *Coord. Chem. Rev.*, 2012, **256**, 2521–2529.

16 S. Chen and L.-W. Wang, *Chem. Mater.*, 2012, **24**, 3659–3666.

17 F. Puntoriero, G. La Ganga, A. Sartorel, M. Carraro, G. Scorrano, M. Bonchio and S. Campagna, *Chem. Commun.*, 2010, **46**, 4725–4727.

18 N. Kaveevivitchai, R. Chitta, R. Zong, M. El Ojaimi and R. P. Thummel, *J. Am. Chem. Soc.*, 2012, **134**, 10721–10724.

19 A. Savini, P. Belanzoni, G. Bellachioma, C. Zuccaccia, D. Zuccaccia and A. Macchioni, *Green Chem.*, 2011, **13**, 3360–3374.

20 D. J. Wasylenko, R. D. Palmer and C. P. Berlinguette, *Chem. Commun.*, 2013, **49**, 218–227.

21 J. L. Boyer, J. Rochford, M.-K. Tsai, J. T. Muckerman and E. Fujita, *Coord. Chem. Rev.*, 2010, **254**, 309–330.

22 L. Duan, F. Bozoglian, S. Mandal, B. Stewart, T. Privalov, A. Llobet and L. Sun, *Nat. Chem.*, 2012, **4**, 418–423.

23 E. A. Karlsson, B.-L. Lee, T. Åkermark, E. V. Johnston, M. D. Kärkäs, J. Sun, Ö. Hansson, J.-E. Bäckvall and B. Åkermark, *Angew. Chem., Int. Ed.*, 2011, **50**, 11715–11718.

24 J. J. Concepcion, J. W. Jurss, P. G. Hoertz and T. J. Meyer, *Angew. Chem., Int. Ed.*, 2009, **48**, 9473–9476.

25 S. M. Barnett, K. I. Goldberg and J. M. Mayer, *Nat. Chem.*, 2012, **4**, 498–502.

26 M.-T. Zhang, Z. Chen, P. Kang and T. J. Meyer, *J. Am. Chem. Soc.*, 2013, **135**, 2048–2051.

27 M. L. Rigsby, S. Mandal, W. Nam, L. C. Spencer, A. Llobet and S. S. Stahl, *Chem. Sci.*, 2012, **3**, 3058–3062.

28 M. Wang, L. Chen and L. Sun, *Energy Environ. Sci.*, 2012, **5**, 6763–6778.

29 K. Sakai and H. Ozawa, *Coord. Chem. Rev.*, 2007, **251**, 2753–2766.

30 V. Artero, M. Chavarot-Kerlidou and M. Fontecave, *Angew. Chem., Int. Ed.*, 2011, **50**, 7238–7266.

31 M. L. Helm, M. P. Stewart, R. M. Bullock, M. R. DuBois and D. L. DuBois, *Science*, 2011, **333**, 863–866.

32 S. Fukuzumi, T. Kobayashi and T. Suenobu, *Angew. Chem., Int. Ed.*, 2011, **50**, 728–731.

33 T. Stoll, M. Gennari, I. Serrano, J. Fortage, J. Chauvin, F. Odobel, M. Rebarz, O. Poizat, M. Sliwa, A. Deronzier and M.-N. Collomb, *Chem.–Eur. J.*, 2013, **19**, 782–792.

34 E. S. Andreiadis, P.-A. Jacques, P. D. Tran, A. Leyris, M. Chavarot-Kerlidou, B. Jousselme, M. Matheron, J. Pécaut, S. Palacin, M. Fontecave and V. Artero, *Nat. Chem.*, 2013, **5**, 48–53.

35 S. Varma, C. E. Castillo, T. Stoll, J. Fortage, A. G. Blackman, F. Molton, A. Deronzier and M.-N. Collomb, *Phys. Chem. Chem. Phys.*, 2013, **15**, 17544–17552.

36 C. Costentin, S. Drouet, G. Passard, M. Robert and J. M. Saveant, *J. Am. Chem. Soc.*, 2013, **135**, 9023–9031.

37 J. M. Smieja, E. E. Benson, B. Kumar, K. A. Grice, C. S. Seu, A. J. M. Miller, J. M. Mayer and C. P. Kubiak, *Proc. Natl. Acad. Sci. U. S. A.*, 2012, **109**, 15646–15650.

38 J. A. Keith, K. A. Grice, C. P. Kubiak and E. A. Carter, *J. Am. Chem. Soc.*, 2013, **135**, 15823–15829.

39 W. Wang, S. Wang, X. Ma and J. Gong, *Chem. Soc. Rev.*, 2011, **40**, 3703–3727.

40 M. S. Jeletic, M. T. Mock, A. M. Appel and J. C. Linehan, *J. Am. Chem. Soc.*, 2013, **135**, 11533–11536.

41 E. E. Benson, C. P. Kubiak, A. J. Sathrum and J. M. Smieja, *Chem. Soc. Rev.*, 2009, **38**, 89–99.

42 J. D. Froehlich and C. P. Kubiak, *Inorg. Chem.*, 2012, **51**, 3932–3934.

43 P. Kang, T. J. Meyer and M. Brookhart, *Chem. Sci.*, 2013, **4**, 3497–3502.

44 C. D. Windle and R. N. Perutz, *Coord. Chem. Rev.*, 2012, **256**, 2562–2570.

45 Y. Tamaki, T. Morimoto, K. Koike and O. Ishitani, *Proc. Natl. Acad. Sci. U. S. A.*, 2012, **109**, 15673–15678.

46 W. J. Youngblood, S.-H. A. Lee, Y. Kobayashi, E. A. Hernandez-Pagan, P. G. Hoertz, T. A. Moore, A. L. Moore, D. Gust and T. E. Mallouk, *J. Am. Chem. Soc.*, 2009, **131**, 926–927.

47 L. Li, L. Duan, Y. Xu, M. Gorlov, A. Hagfeldt and L. Sun, *Chem. Commun.*, 2010, **46**, 7307–7309.

48 Y. Gao, X. Ding, J. Liu, L. Wang, Z. Lu, L. Li and L. Sun, *J. Am. Chem. Soc.*, 2013, **135**, 4219–4222.

49 L. Li, L. Duan, F. Wen, C. Li, M. Wang, A. Hagfeldt and L. Sun, *Chem. Commun.*, 2012, **48**, 988–990.

50 Z. Ji, M. He, Z. Huang, U. Ozkan and Y. Wu, *J. Am. Chem. Soc.*, 2013, **135**, 11696–11699.